

First Annual Report

on

Dielectric Studies of the Cation Substituted  
Mixed Crystals of Niobates

Period Covered: June 1, 1968 - June 1, 1969

By: Franklin F. Y. Wang

Prepared for

National Aeronautics and Space Administration

Washington, D. C. 20546

Contract Monitors: Mr. Howard Lessoff, RMM

Dr. Philipp H. Klein, RMM

## Table of Contents

<u>Section</u>	<u>Page</u>
I. ABSTRACT	1
II. DISCUSSION	1
A. Objective	1
B. Sample Preparations	3
C. Sample Preparations	5
1. Lattice parameters	5
2. Linear thermal expansion	8
3. Dielectric constant	15
4. Electrical conductivity	16
D. Related Activities:	23
1. Presented talks	23
2. Submitted papers	26
III. FUTURE PLANS	27
IV: ACKNOWLEDGEMENT	27
Appendix A. Design and Construction of a Dilatometer for the Temperature Range of 300°K to 1000°K.	29
Appendix B. Operation and Calibration of a Dilatometer.	30
Appendix C. Abstracts of Presented Talks	31
Appendix D. Empirical Factors for Calculation of the Ferro- Electric Transition Temperatures of Tungsten Bronze Type Niobates.	33

## List of Illustration

<u>Figure</u>		<u>Page</u>
1	Photomicrograph of thermally etched sample No. B-0-3, $Ba_2NaNb_5O_{15}$ . 500 x magnification.	6
2	Linear thermal expansion vs. temperature of sample B-0-3, $Ba_2NaNb_5O_{15}$ .	9
3	Linear thermal expansion vs. temperature of sample B-4-3, $Ba_{1.9}Gd_{0.1}Na_{1.0}Nb_5O_{15.05}$ .	10
4	Linear thermal expansion vs. temperature of sample A-5-3, $Ba_{2.0}Gd_{0.1}Na_{0.9}Nb_5O_{15.10}$ .	11
5.	Linear thermal expansion vs. temperature of sample B-6-3, $Ba_{1.95}Gd_{0.1}Na_{0.95}Nb_5O_{15.075}$ .	12
6.	Linear thermal expansion curves, of samples B-0-3 and B-6-3 on expanded temperature scales.	13
7.	Linear thermal expansion curves of samples A-5-3, and B-4-3 on expanded temperature scales.	14
8.	Dielectric constant vs. frequency for samples C-0-3, A-4-3, A-5-3, and A-6-3 at room temperature.	17
9.	Dissipation factor vs. frequency for samples C-0-3, A-4-3, A-5-3, and A-6-3 at room temperature.	13
10.	High temperature dielectric measuring setup - vacuum housing assembly.	19
11.	High temperature dielectric measuring setup - sample holder, parts A and B.	20

Figure

Page

- 12. High temperature dielectric measuring setup - sample holder, part C. 21
- 13. High temperature dielectric measuring setup - exploded view of sample holder. 22
- 14. Logarithm of electrical conductivity vs. 1/T for sample B-0-3,  $Ba_2NaNb_5O_{15}$ . 24
- 15. Logarithm of electrical conductivity vs. 1/T for sample B-0-3,  $Ba_2NaNb_5O_{15}$ . 25



## I. Abstract:

The preparation and compositions of Gd-substituted  $\text{Ba}_2\text{NaNb}_5\text{O}_{15}$  is discussed. The properties under study included the lattice parameters, density, linear thermal expansion, dielectric constant, microstructure, and electrical conductivity. Some of the measuring setups are described and discussed. From the linear thermal expansion data, phase transitions were shown in these niobate samples. An approach, which related empirical factors of cations with the ferroelectric transition temperatures, is included in the Appendix.

## II. Discussion:

### A. Objective

The objective of this program is to study the dielectric properties of ceramic mixed crystals (solid solutions) containing barium sodium niobate  $\text{Ba}_2\text{NaNb}_5\text{O}_{15}$ ; to correlate the "intrinsic" dielectric properties with the chemical compositions; to correlate the "extrinsic" dielectric properties with the composition and the microstructure of the samples; and to devise appropriate means to improve the dielectric properties.

This study departs from the usual practices of isostructural substitutions in preparing the mixed crystals. Common practices substitute a cation A by another cation B, where A and B have the same ionic charge and the ionic sizes of A and B differ by less than 15%. Such practices have the advantage of maintaining the crystal structure of unsubstituted compound. But, they tend to obscure the intrinsic properties due to cation substitution from the extrinsic

properties of the samples, as the former effect becomes either equal to or less than the latter effect. This study takes a drastic path in selecting a substituting cation which is different both in its ionic size and ionic charge from the substituted cation. The substituting cation species, selected for initial study, is gadolinium Gd, and it is used to substitute for barium Ba, or sodium Na, or both. Sodium is monovalent, barium is di-valent, and Gd is trivalent. Their ionic sizes are 0.98 Å, 0.99 Å, and 1.43 Å for Na<sup>+</sup>, Gd<sup>3+</sup> and Ba<sup>2+</sup>, respectively. It is therefore obvious that the Gd substitution will provide significant differences from Ba<sub>2</sub>NaNb<sub>5</sub>O<sub>15</sub>. Furthermore, the substituted cations, either Ba, or Na, or both, will produce some differences too. Using this approach, it is thought that we can, first of all, deal only with the "intrinsic" properties brought about by the Gd substitution. Those "extrinsic" properties such as grain size effect, porosity effect etc., which are the results of sample preparation, are at present studied in a secondary role.

There are infinite combinations of Gd substitution to Ba<sub>2</sub>NaNb<sub>5</sub>O<sub>15</sub>. We first limit ourselves to one strong constraint, namely, 0.1 moles of cations in Ba<sub>2</sub>NaNb<sub>5</sub>O<sub>15</sub> are substituted in each case.

We then limit ourselves to six ways of substitution. They are:

<u>No</u>	<u>Composition</u>
0	$Ba_2NaNb_5O_{15}$
4	$Ba_{1.9}Gd_{0.1}Na_{1.0}Nb_5O_{15.05}$
5	$Ba_{2.0}Gd_{0.1}Na_{0.9}Nb_5O_{15.10}$
6	$Ba_{1.95}Gd_{0.1}Na_{0.95}Nb_5O_{15.075}$
13	$Ba_{1.9}Gd_{0.05}Na_{1.05}Nb_5O_{15}$
14	$Ba_{2.0}Gd_{0.0334}Na_{0.9}Nb_5O_{15}$
15	$Ba_{1.95}Gd_{0.05}Na_{0.95}Nb_5O_{15}$

In all these compositions, the chemical formulae given are the theoretical or ideal formulae. The actual compositions may contain either cation vacancies or oxygen vacancies or both. However, from the ideal formulae, the compositions Nos. 4,5 and 6 represent nonstoichiometric compositions. In them, the mole number for the total cations remains the same, i.e., 3. Because of the different valence for Gd as for Ba or Na, the mole number of oxygen must therefore deviate from its original number, i.e., 15. On the other hand, the compositions Nos. 13,14 and 15 represent stoichiometric compositions. They are made according to the strong constraint. (The composition No. 13 violated this rule, however).

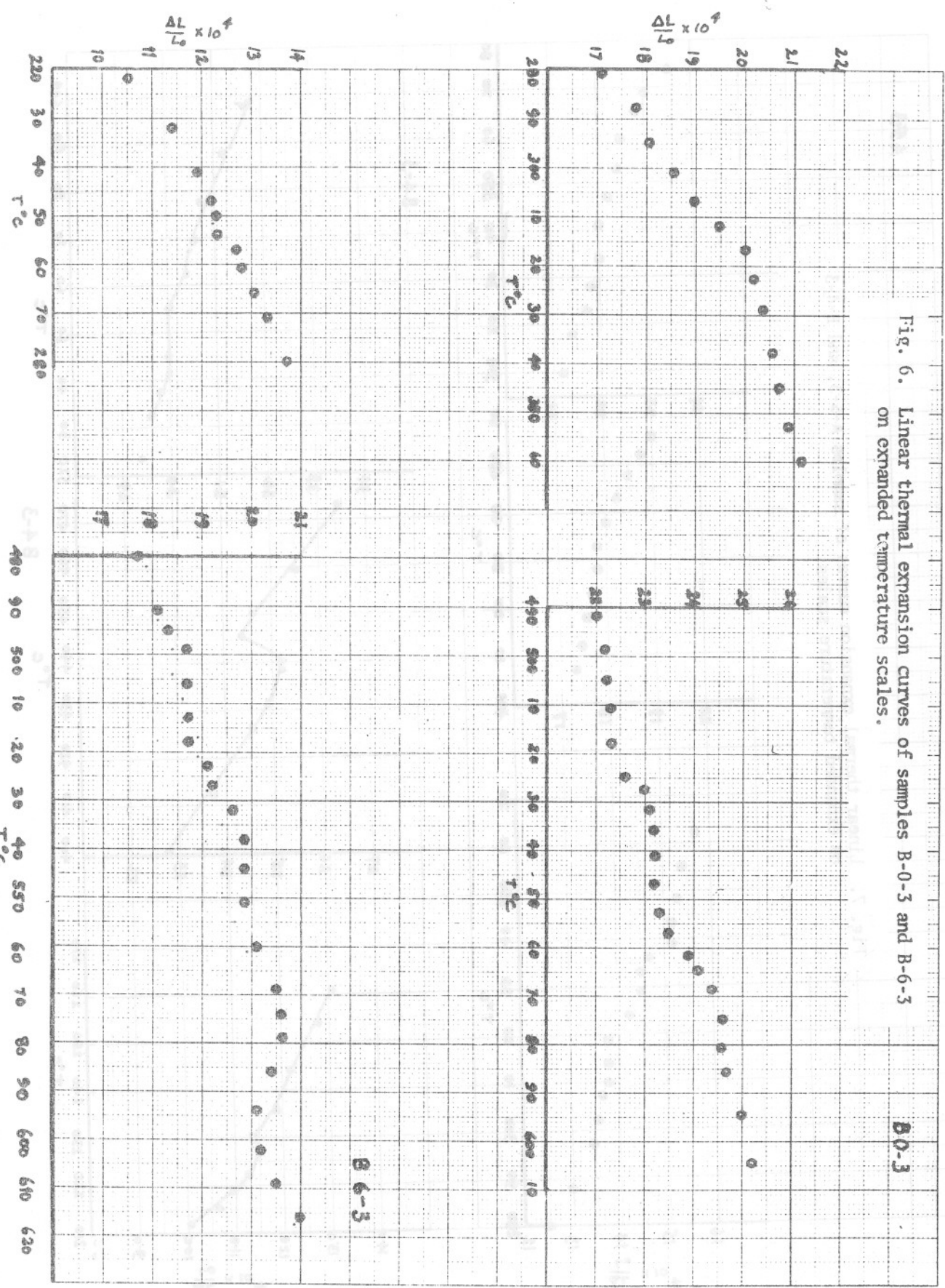
B. Sample preparations:

Raw materials used in this study are:  $BaCO_3$  (reagent grade, Fisher),  $Na_2CO_3$  (reagent grade, Fisher),  $Gd_2O_3$  (American Potash code 929.9), and  $Nb_2O_5$  (Kewacki, optical grade). Each batch was

about 20 grams in weight. Mixing of raw materials was done by hand with an agate mortar and pestle. Methyl alcohol was used as the mixing and grinding medium. Drying was done with an infrared lamp. Pellets of 1 inch diameter and 1/4 inch height were pressed from the dried powders. They weighed about 10 grams each. The pellets were placed on a 10 mil platinum foil and dried in a globar resistance heating furnace in ambient atmosphere. The furnace was controlled by a proportional temperature controller (Temp-Tendor, API) to within  $\pm 5^{\circ}\text{C}$ . Pellets were placed into the furnace below  $100^{\circ}\text{C}$ . The furnace reached  $1200^{\circ}\text{C}$  in about 24 hours. The pellets were maintained at  $1210^{\circ} \pm 5^{\circ}\text{C}$  for 16 to 18 hours. After which, the power was turned off, and the pellets were furnace-cooled to about  $100^{\circ}\text{C}$  in about 10 hours. The fired pellets were crushed by hand to powders. X-ray diffraction runs were made on the powder samples to insure complete chemical reactions. If the x-ray results indicated incomplete reactions, a re-firing of the powders in pellet form was made. In most cases, single firing was sufficient.

For samples used in physical measurements, they were cold-pressed in a Carver laboratory press. A 1/2" die was used. The samples were then fired in the same firing and cooling schedule as the first firing. Fired samples, after fine mechanical polishings, were used for dielectric and electrical conductivity measurements. The samples used for dilatometer were cut from the pellets into sizes

Fig. 6. Linear thermal expansion curves of samples B-0-3 and B-6-3 on expanded temperature scales.



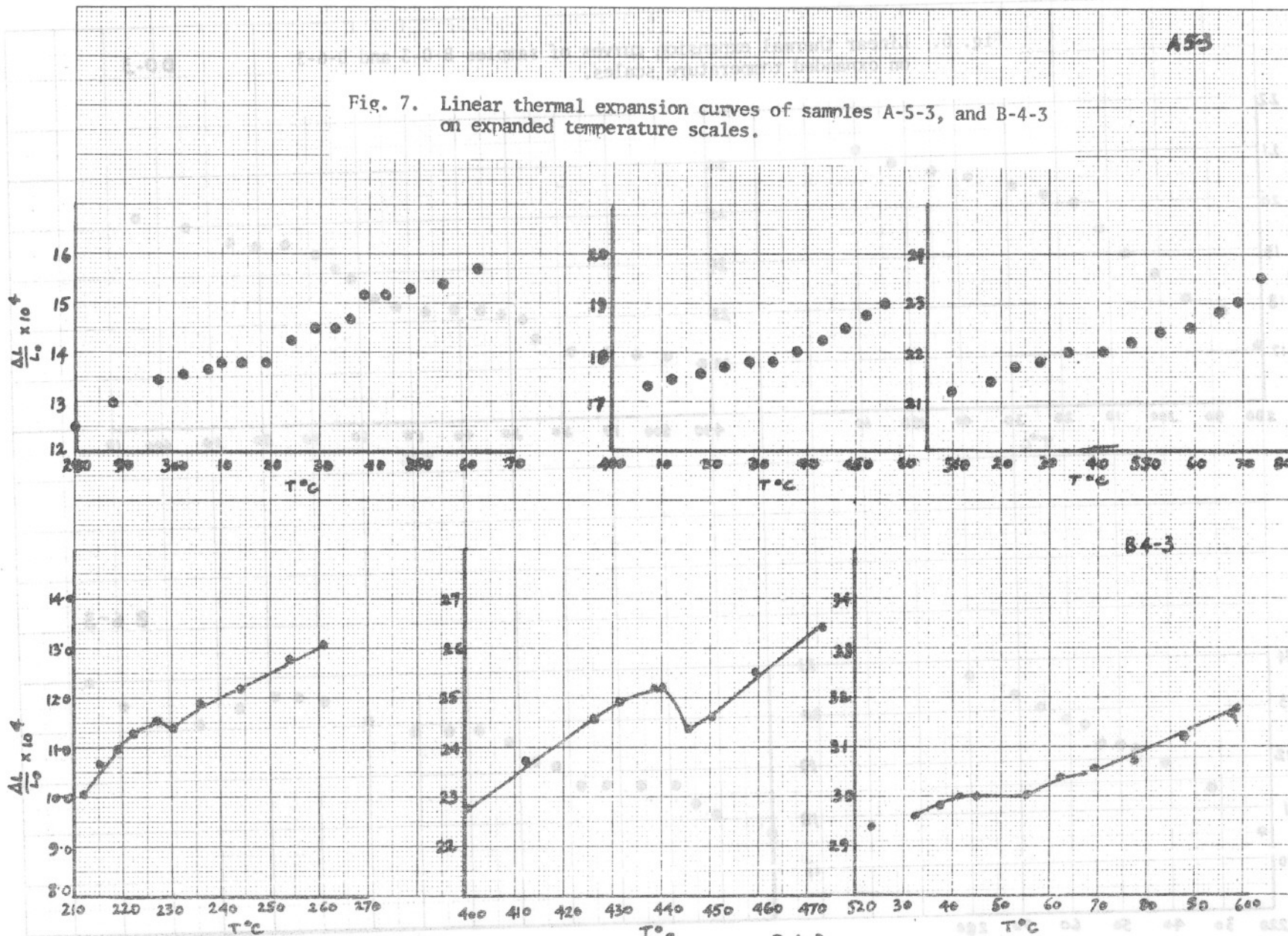
EUGENE DIETZEN CO.  
MADE IN U. S. A.

DIETZEN GRAPH PAPER  
MILLIMETER  
NO. 34-D-M-3-H-3



A53

Fig. 7. Linear thermal expansion curves of samples A-5-3, and B-4-3 on expanded temperature scales.



B4-3

a detectability in  $\Delta L/L_0$  of  $0.3 \times 10^{-4}$ . At the present time, we are still in the process of ascertaining which of these changes are truly phase transition behaviors. On the other hand, as shown in Appendix B, the linear thermal expansion curves of ferrite sample did not show sharp changes in slope, therefore, they are definitely not due to spurious responses of the dilatometer.

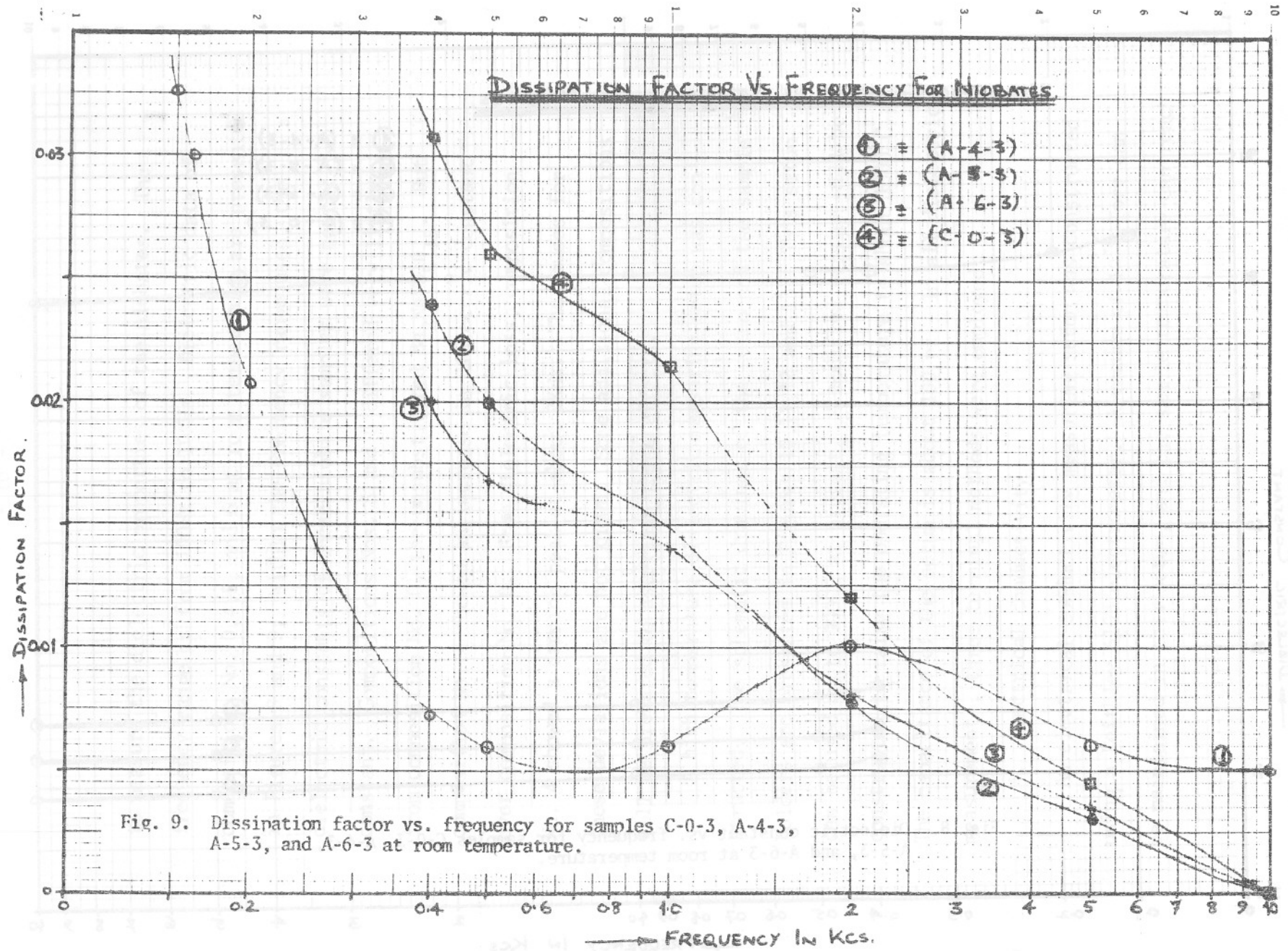
We can only identify the temperature regions where the slope change behaviors occurred. They are as follows:

<u>Composition No.</u>	<u>Slope changing regions</u>
0	310° - 330°C; 510° - 540°C; 540 - 570°C; 570° - 600°C
4	220° - 250°C; 430° - 460°C; 540° - 570°C
5	310° - 350°C; 420° - 450°C; 520° - 550°C
6	220° - 240°C; 430° - 460°C; 530° - 570°C

The ferroelectric Curie temperature  $T_c$  of  $Ba_2NaNb_5O_{15}$  (composition No. 0) was reported to be 560°C (L.G. Van Uitert et al, Mat. Res. Bull. 3, 47 (1968)). These behaviors are being carefully studied currently.

### 3. Dielectric constant

A General Radio type 1620-A capacitance-measuring assembly, together with a General Radio Dielectric Sample Holder, was used





SAMPLE HOLDER

### VACUUM TUBE ASSEMBLY

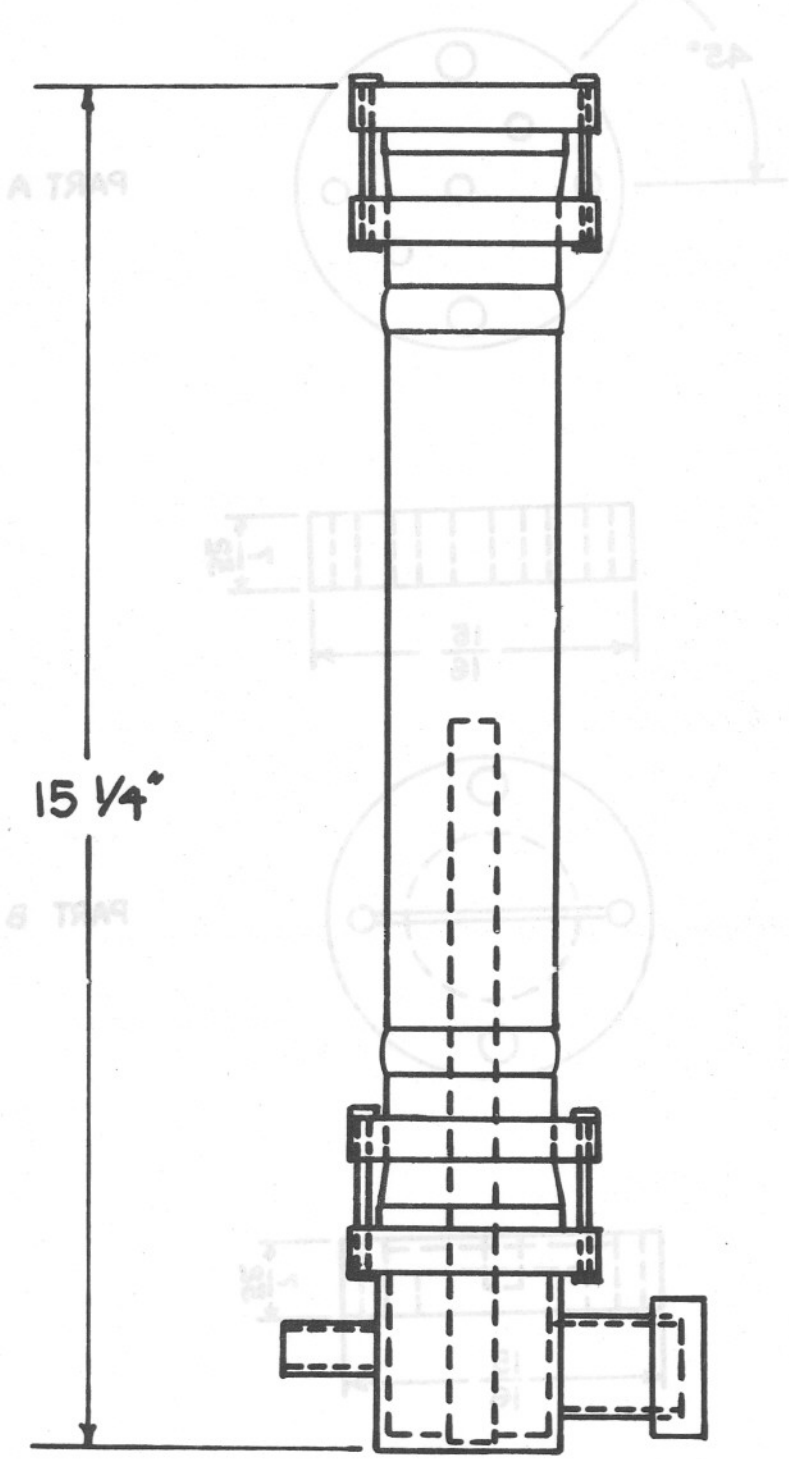


Fig.10. High temperature dielectric measuring setup - vacuum housing assembly.

# SAMPLE HOLDER

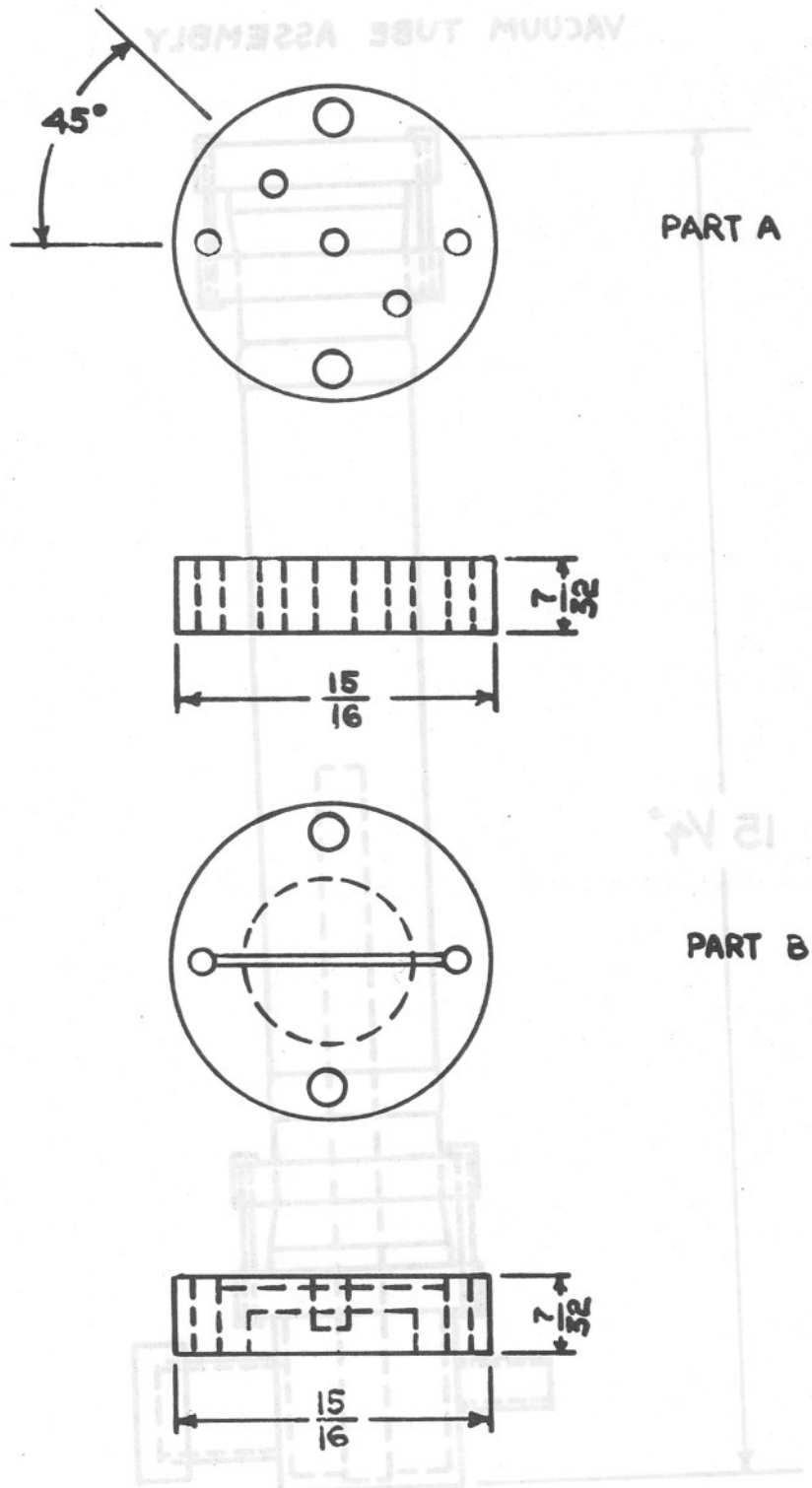


Fig.11. High temperature dielectric measuring setup - sample holder, parts A and B.

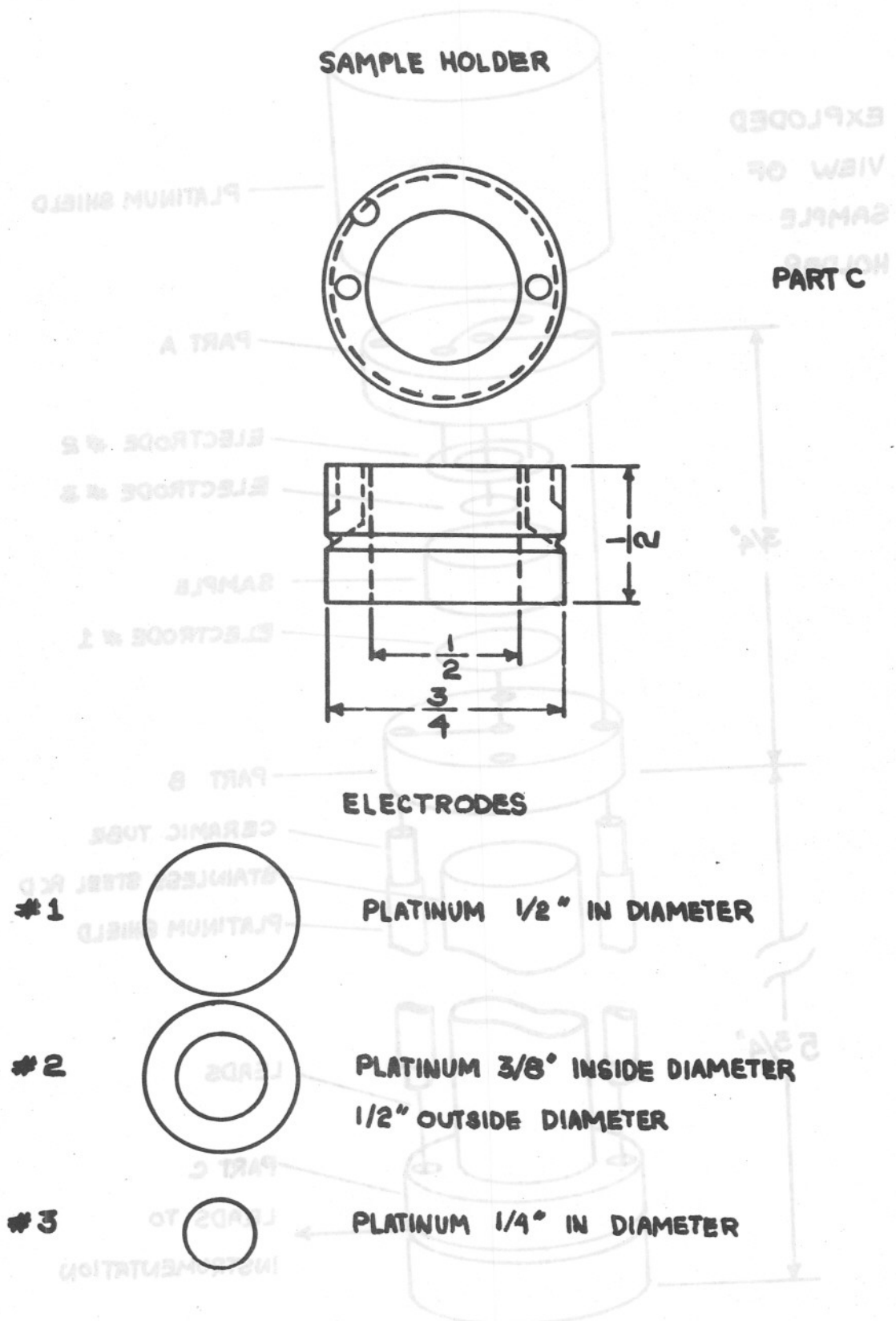


Fig.12. High temperature dielectric measuring setup - sample holder, part C.

**EXPLODED  
VIEW OF  
SAMPLE  
HOLDER**

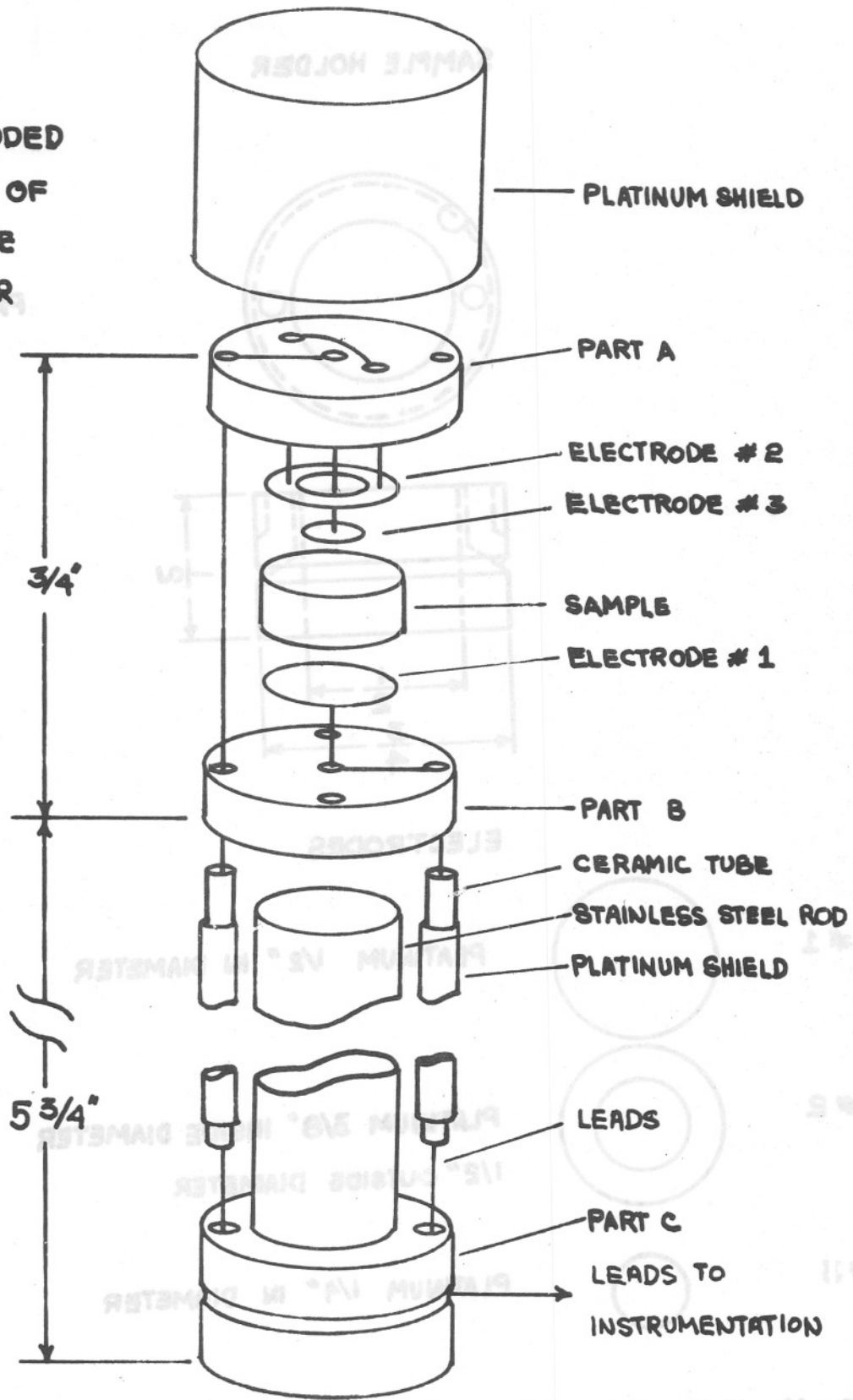


Fig.13. High temperature dielectric measuring setup - exploded view of sample holder.

1000°C. A plot of  $\ln \sigma$  vs.  $1/T$  for sample No. B-0-3, unsubstituted  $\text{Ba}_2\text{NaNb}_5\text{O}_{15}$ , is shown as Figure 14, where  $\sigma$  is the conductivity. The activation energies were found to be 0.51 eV between 600°C-800°C, 1.14 eV between 300°C-425°C, and 0.79 eV between 160°C-300°C, respectively. It is interesting to note that in the temperature regions which we reported changes of slopes in the linear thermal expansion curves, there are also changes of slopes in the conductivity curves. These regions are marked with arrows in Figure 14.

Tests will be conducted at different partial oxygen pressures in order to establish the intrinsic region of the electronic conduction. From it, we can learn about the non-stoichiometries of our samples.

D. Related activities:

1. Presented talks

A talk, entitled "Empirical Factors for Calculations of the Ferroelectric Transition Temperatures of Tungsten Bronze Type Niobates", was presented before the meetings of the American Physical Society, March, 1969.

A talk, entitled "Elastic Moduli of Binary Composites", was presented before the meetings of the American Ceramic Society, May, 1969.

The abstracts of both talks are included in Appendix C.

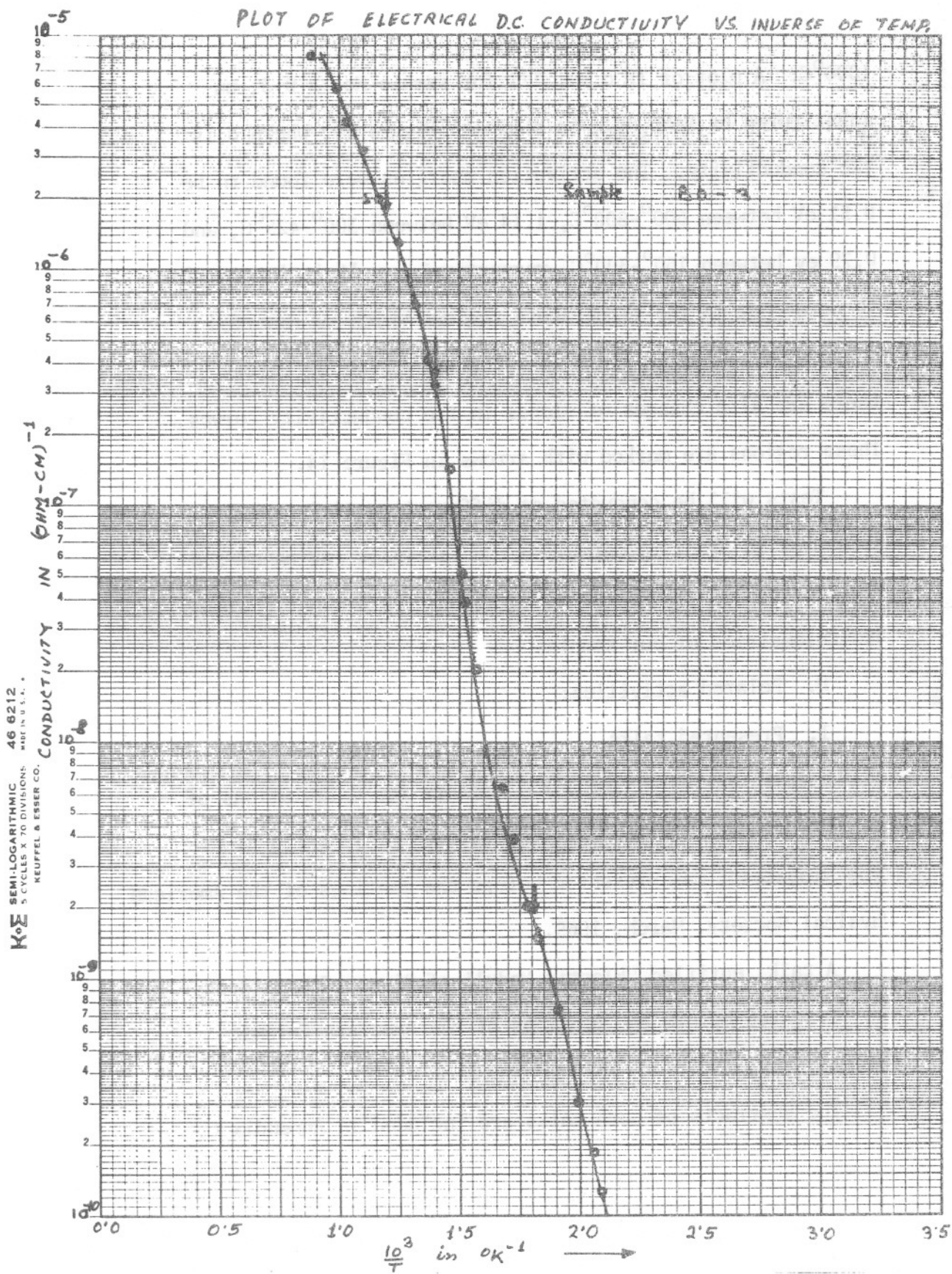
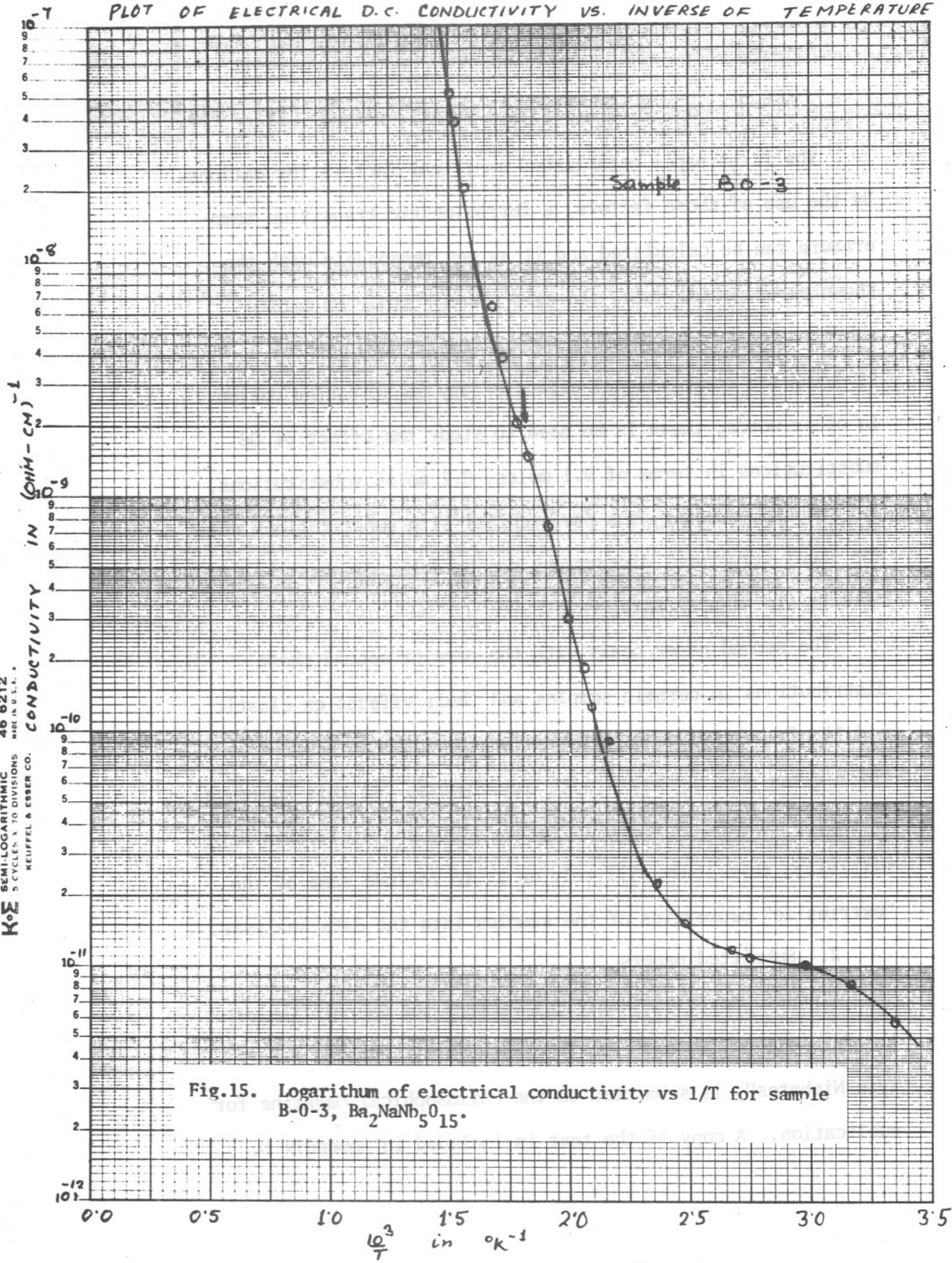


Fig.14. Logarithm of electrical conductivity vs 1/T for sample B-0-3,  $Ba_2NaNb_5O_{15}$ .



PLOT OF ELECTRICAL D.C. CONDUCTIVITY VS. INVERSE OF TEMPERATURE



The first paper established empirical factors for cations. By the use of these factors, a ferroelectric transition temperature can be calculated and it agrees reasonably with the known experimental data. In this present study of cation substitutions, this approach will eliminate the need of studying the compositional effect of any substituting cation. In other words, there is no need to study the effect of Gd substitutions in terms of 0.1 moles, 0.2 moles substitutions, and so on. Moreover, the preferential site substitutions and the local structural distortions can be detected when the effects are significant.

The second paper deals with the pore or second phase distributions in ceramic samples and their effects on elastic moduli of the samples. A statistical approach is adopted which gives good agreement with experiments. As this approach is easily adapted to magnetic permeability and dielectric permittivity, this study will rely on it to include some of the "extrinsize" properties of the samples into the data analysis.

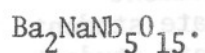
## 2. Submitted papers

A paper, entitled "Empirical Factors for Calculation of the Ferroelectric Transition Temperatures of Tungsten Bronze Type Niobates", is submitted to the Philosophical Magazine for publication. A copy of the text is included in Appendix D.

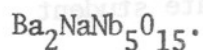


### III. Future Plans:

A. We will continue the study of Gd substitutions into



B. We will also study the effect of Cr substitutions into



C. We will continue the study based on these properties:

1. Lattice parameters
2. Density
3. Microstructure
4. Linear thermal expansion
5. Dielectric constant
6. Electrical conductivity

D. We have initiated an electron microprobe analysis of the niobate samples. We plan to use this approach for the following features:

1. The chemical homogeneity of the ceramic sample as prepared.
2. The homogeneity of Gd, or other cation, substitutions in the sample.

E. We plan to make some correlations between the cation substitutions from the structural viewpoint with their dielectric properties.

### IV. Acknowledgement

The progress of this project has been contributed in various degrees by many personnels, whose names are listed in the following:

Jahar L. Mukherjee	Graduate student
Kedar Gupta	Graduate student
Chandra Khattak	Graduate student
Charles Faber	Undergraduate student
Richard LeLong	Undergraduate student
John Clukies	Undergraduate student
Siegfried Esslinger	Undergraduate student
Walter Werner	Undergraduate student

Their efforts are hereby gratefully acknowledged. In addition, the technical assistances of Mr. Frank Merkert are indispensable to this project. The advices and encouragements from the project monitors, Mr. Howard Lessoff, and Dr. Philipp H. Klein, NASA-ERC are also gratefully acknowledged. They have contributed substantially to this project. The expert assistance from our secretary, Miss Bernadette Munro, is also gratefully acknowledged.

ABSTRACT

The dilatometer is used to measure the linear thermal expansion of solid materials. The dilatometer constructed and used in this experiment has the special feature of being able to be used from 300°K to 1000°K without removing the sample although for our purposes here, only the high temperature case will be considered. The use of a linear Variable Differential Transformer (VDT) to convert a change in length of the sample to an electrical signal input to a millivolt recorder. A furnace capable of reaching 1000°K was constructed and used for the experiment.

APPENDIX A

DESIGN AND CONSTRUCTION OF A DILATOMETER  
FOR THE TEMPERATURE RANGE OF 300° K TO 1000° K

BY CHARLES FABER AND  
RICHARD LELONG

The Kenthal wire was wound on the core so as to give a non-inductive coil as shown in the following diagram:

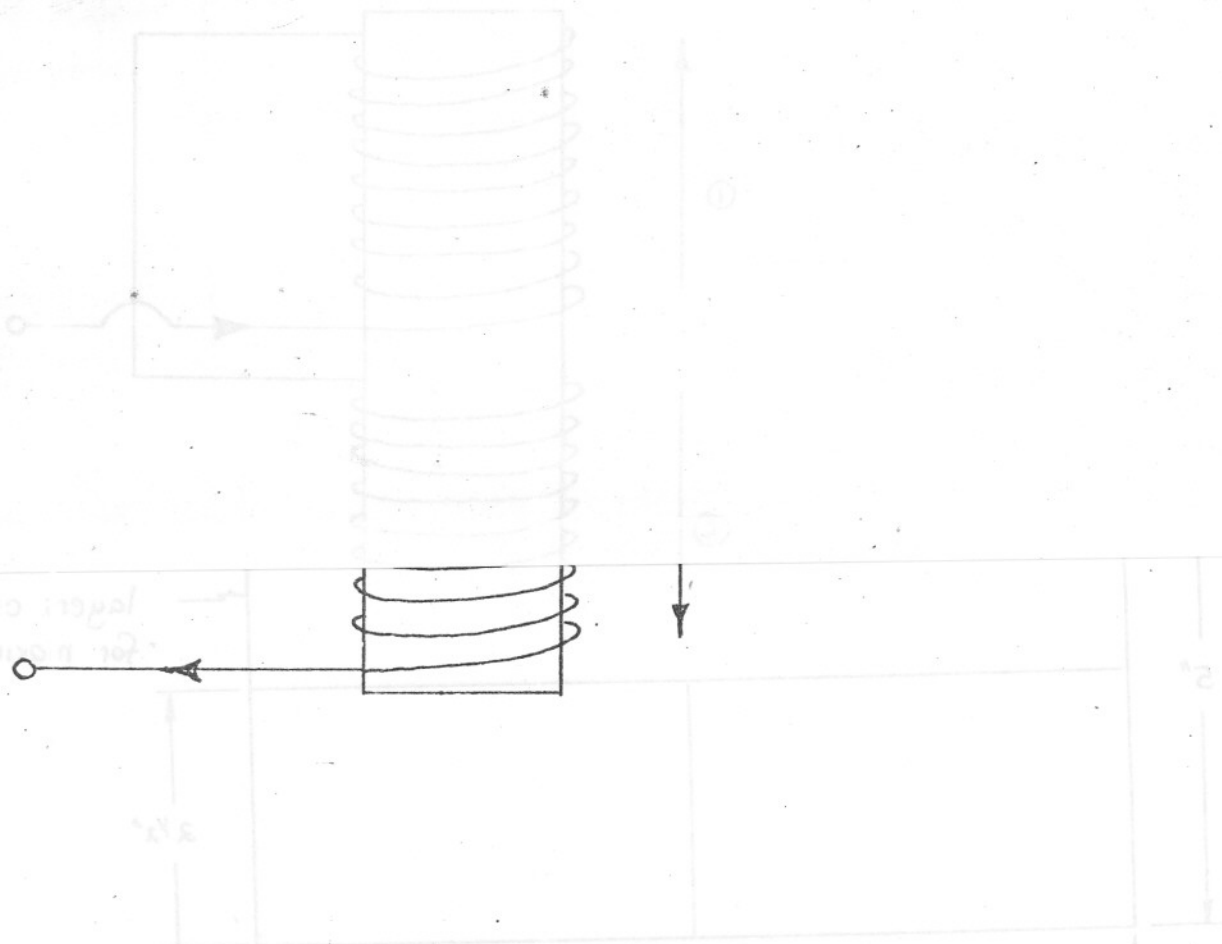
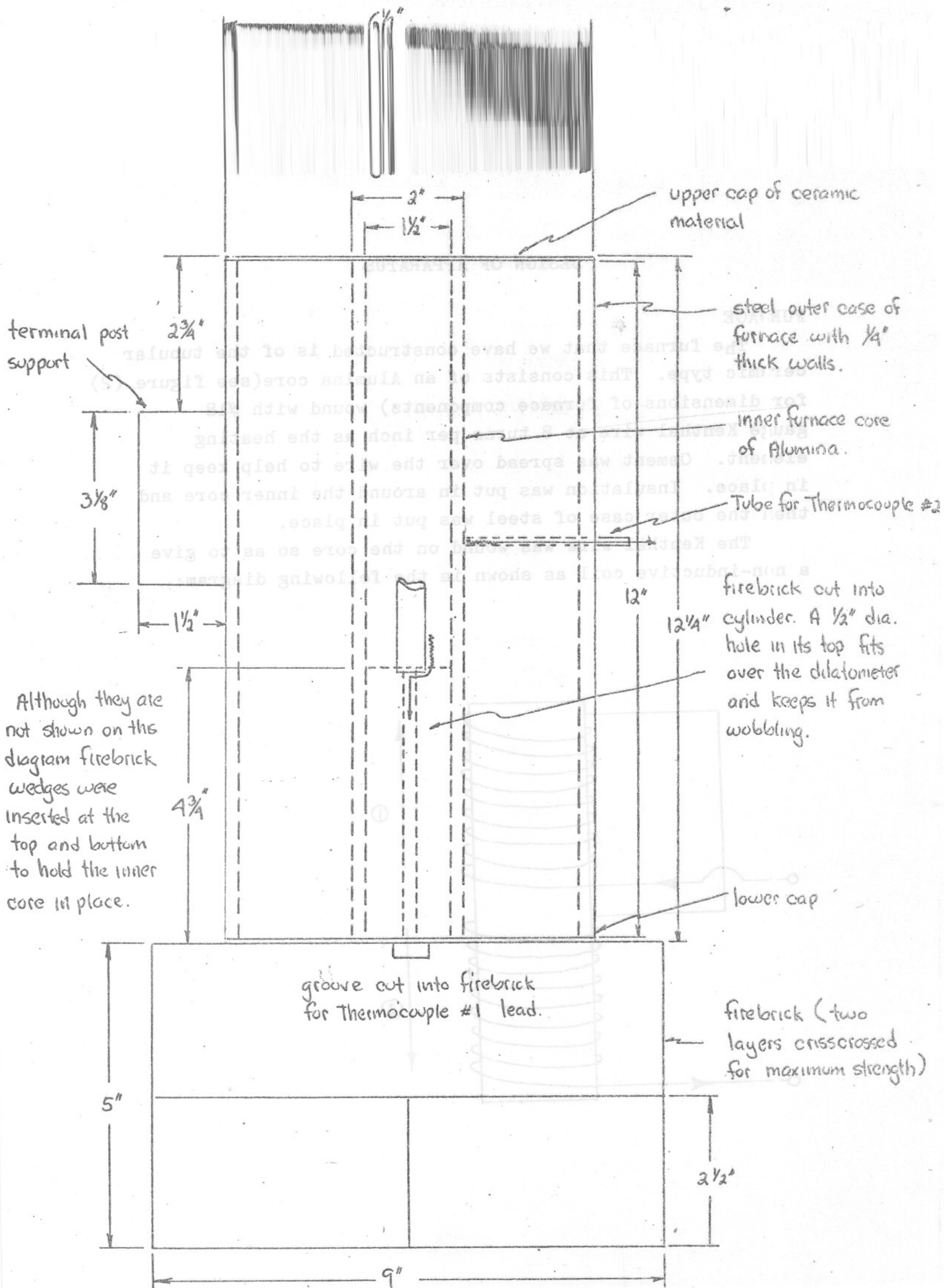


DIAGRAM OF FURNACE (1/2 SCALE)



## PRINCIPLE OF OPERATION

Figure (1) shows a block diagram of the entire experimental setup. The construction of the furnace and dilatometer will be discussed in detail in the next section.

The variac is used to supply a variable power source to the furnace. This variac has a voltage of 0-140 volts and a current capacity of 10 amps. (See Appendix A for a complete list of instruments and specifications). A time proportional controller is inserted in the setup between the variac and the wall outlet to control the inside furnace temperature through the use of thermocouple #2. The time proportional controller can be preset to a given temperature at which the furnace is desired to remain. When this temperature is reached, the controller cuts off the power to the variac. As the furnace begins to fall below the preset temperature the power is restored to the variac. In this manner, the time proportional controller maintains a constant temperature inside the furnace.

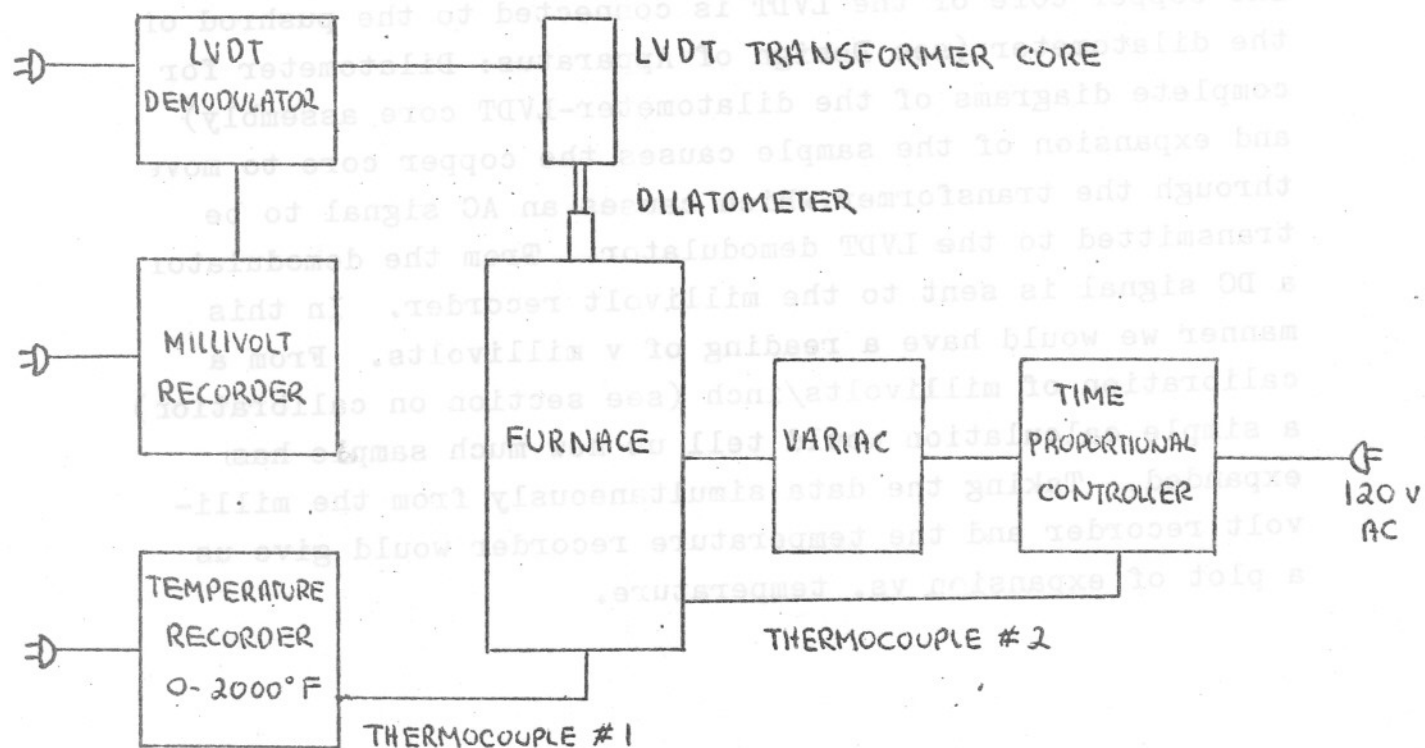


FIGURE (1)

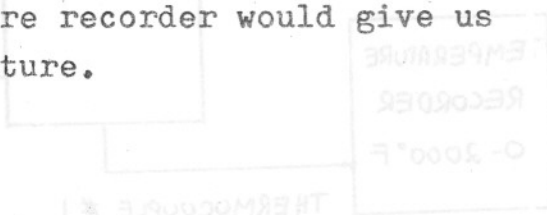
PRINCIPLES OF OPERATION

A useful feature of the controller is that it can also be used to increase or decrease the furnace temperature at a specified rate. For our purposes, however, we will not be taking advantage of this feature at this time. Further experiments using this setup may prove interesting.

The furnace is of tubular ceramic type. It was designed to give a constant temperature range over a sample about  $\frac{1}{2}$ " long and  $\frac{1}{8}$ " in diameter. The design and construction of the furnace is discussed fully in the next section.

An Easterline Angus temperature recorder with a scale reading from 0-2000°F is used to record the temperature inside the furnace. A chromel-alumel thermocouple is positioned next to the sample and the leads extend down and out the bottom of the furnace and over to the temperature recorder. The cold junction temperature is assumed to be at room temperature.

The dilatometer is positioned in the furnace such that the sample is approximately in the center of the furnace. The copper core of the LVDT is connected to the pushrod of the dilatometer (see Design of Apparatus: Dilatometer for complete diagrams of the dilatometer-LVDT core assembly) and expansion of the sample causes the copper core to move through the transformer, which causes an AC signal to be transmitted to the LVDT demodulator. From the demodulator a DC signal is sent to the millivolt recorder. In this manner we would have a reading of v millivolts. From a calibration of millivolts/inch (see section on calibration) a simple calculation would tell us how much sample has expanded. Taking the data simultaneously from the millivolt recorder and the temperature recorder would give us a plot of expansion vs. temperature.



TEMPERATURE RECORDER  
0-2000°F

MILLIVOLT RECORDER

LVDT DEMODULATOR



In the top portion of the coil the magnetic field induced by the current flow is in the direction of arrow 1. In the lower portion of the coil the magnetic field is in the direction indicated by arrow 2. These two fields will tend to cancel each other and in this manner will give a non-inductive coil. From power relationships:

$$P=EI=E^2/R$$

For our coil the resistance was measured to be 20 ohms.

Substituting this value into the power formulas:

$$P=E^2/R=(110^2)/(20)=(1.21 \times 10^4 \text{ volts}^2)/(20 \text{ ohms})=.6 \times 10^3 \text{ watts}$$

.6 x 10<sup>3</sup> watts is still a reasonable power consumption as compared to the .5 x 10<sup>3</sup> watts we had calculated previously in the final plan of the experiment.

$$P=EI$$

$$I=P/E=.6 \times 10^3 \text{ watts}/110 \text{ volts}=5.45 \text{ amps}$$

5.45/10, the amperage requirement is satisfied.

Kenthal wire has a resistance of 800ohms/cir mill/ft. for

#18 gauge Kenthal wire:: 1624 cir. mills.

$$800/1624=.493 \text{ ohms/ft.}$$

$$20 \text{ ohms}/.493=41.0 \text{ ft.}$$

$$C=2\pi R$$

$$R=1"$$

$$C=2\pi=6.28"$$

$$(12 \text{ in./ft.})(41.0 \text{ ft.})=492"$$

$$(8 \text{ turns/in})(6.28)=50.2" \text{ used per inch of core.}$$

$$492/50.2=9.8"$$

This length is the amount of core covered by the Kenthal wire turns. This is reasonable for our furnace since when we were winding the wire on the 12" long alumina core we left approximately 1/2" at both ends and 1" in the middle to anchor the wire windings securely to the core and for leads to extend out.(see "Building the Furnace").

Calculate the heat loss for the furnace

$$\text{Heat loss} = 2\pi k_1 (T-T_1)L/2.3 \log(D/d)$$

$k_i$  = thermal conductivity of insulation = .005 watts/sq.in./in./ C.

$T_1$  = surface temperature

L = length of core

D = outside diameter of furnace

d = inside diameter of core

$$\begin{aligned} \text{Heat loss} &= 2 (.005)(650)(12.25)/2.3 \log(6.5/1.5) \\ &= (6.28)(.005)(650)(12.25)/(2.3)(.64) \\ &= (4.25)(5 \times 10^{-3})(6.5 \times 10^2)(1.225 \times 10)/(1.47) \\ &= (4.25)(5 \times 10^{-3})(6.5 \times 10^2)(1.225 \times 10) \\ &= 170 \text{ watts} \end{aligned}$$

For our own design we had estimated a heat loss of 200 watts. The heat loss for this furnace of 170 watts indicates that this was a somewhat better design. The following is a comparison between the parameters of our first design and the actual furnace as it is ready for the experiment:

	Design	Actual Furnace
D	6.3"	6.5"
d	2"	1.5"
L	11"	12.25"
k	.005	.005
h.l.	200 watts	170 watts



DILATOMETER

The dilatometer was built for us by the glass shop at Brookhaven Laboratory with a few minor modifications to our original specifications. The pushrod was made out of a tube of fused silica rather than a rod. This proved to be an advantage later on when we used the adapter (made by the machine shop) to connect the pushrod to the copper core. Instead of using fused silica beads to keep the pushrod aligned, fused silica rings were slipped over the pushrod and attached to it at various points. (see figure (3)). The adapter was attached to the pushrod by heating the end of the pushrod with a soldering iron and allowing melted wax to diffuse into the pushrod. The adapter was then inserted into the pushrod and the wax allowed to harden. The copper core could then be screwed on and off when necessary.

The dilatometer is constructed of fused silica. Fused silica melts at 1200°K which will necessitate careful operation of the furnace but it also has the advantage of having a low coefficient of linear expansion ( $5.4 \times 10^{-7} / ^\circ\text{C}$  from Materials Handbook). This is of importance since the dilatometer will also be expanding with the sample under study.

The dilatometer consists of a fused silica tube  $1/2''$  in diameter and  $10''$  long. This tube is closed at one end which forms a base for the sample to stand on. At this same end is an opening in the side of the tube which permits the sample to be inserted. A fused silica pushrod extends from the top of the sample up through the tube to the open end at which it is attached to the copper core of the LVDT. The pushrod is  $10 \ 1/2''$  long and  $1/8''$  in diameter. It is of the same diameter as the sample so that the forces of expansion of the sample are distributed evenly over the pushrod.

DIAGRAM OF DILATOMETER (3/4 SCALE)

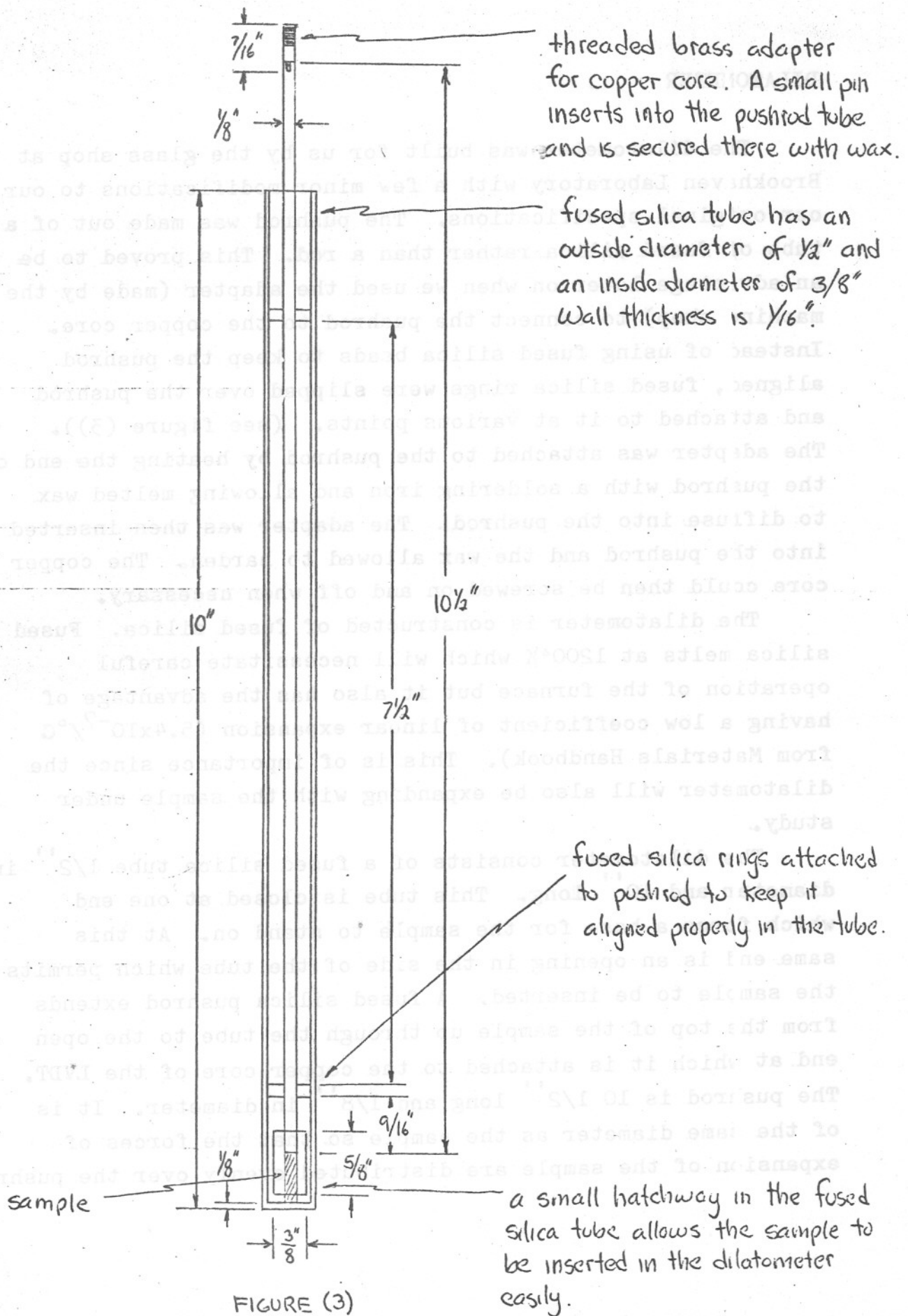


FIGURE (3)

## BUILDING THE FURNACE

Although we have already a section covering the design of the furnace, we feel that a separate section should be devoted to the actual building process and techniques used in the construction of the furnace.

We were fortunate to be able to acquire a second hand furnace from which we made use of the outer case and the insulation. An Alumina core 12" long and with O.D.=2" and I.D.=1½" was readily available and we decided to use this although it was not pregrooved. (We had planned to use the original core but we found it beyond repair when we unwound the old wire). Winding the Kenthal wire on an ungrooved core successfully proved to be almost impossible. To alleviate this condition, we cut grooves in the alumina core, spaced 8 to an inch (see figure 4a).

The Kenthal wire was attached securely to the alumina core by using an 8" piece of Kenthal wire wound over the other wire and drawn tight with pliers. About 24" was left as a lead (see figure 4b). Later on, these leads were folded over on themselves and twisted to decrease the resistance in the leads.

After the Kenthal wire had been wound on the core a thin coat of cement was put on over the wires so that they were just visible. The inner core was then connected to the variac and 30 volts were put across the leads and left over night to dry (see figure 4c). Two layers of firebrick were used to keep the inner core off the table.

When the cement was completely dry, the inner core was placed into the outer case and the bottom cover was put on. Wedges of firebrick were inserted at the top and bottom of the furnace to keep the inner core in place. Insulation was then put in, taking care to leave dead airspaces and

not to pack it too tightly. The top cover was then secured in place and the leads connected to the terminal posts.

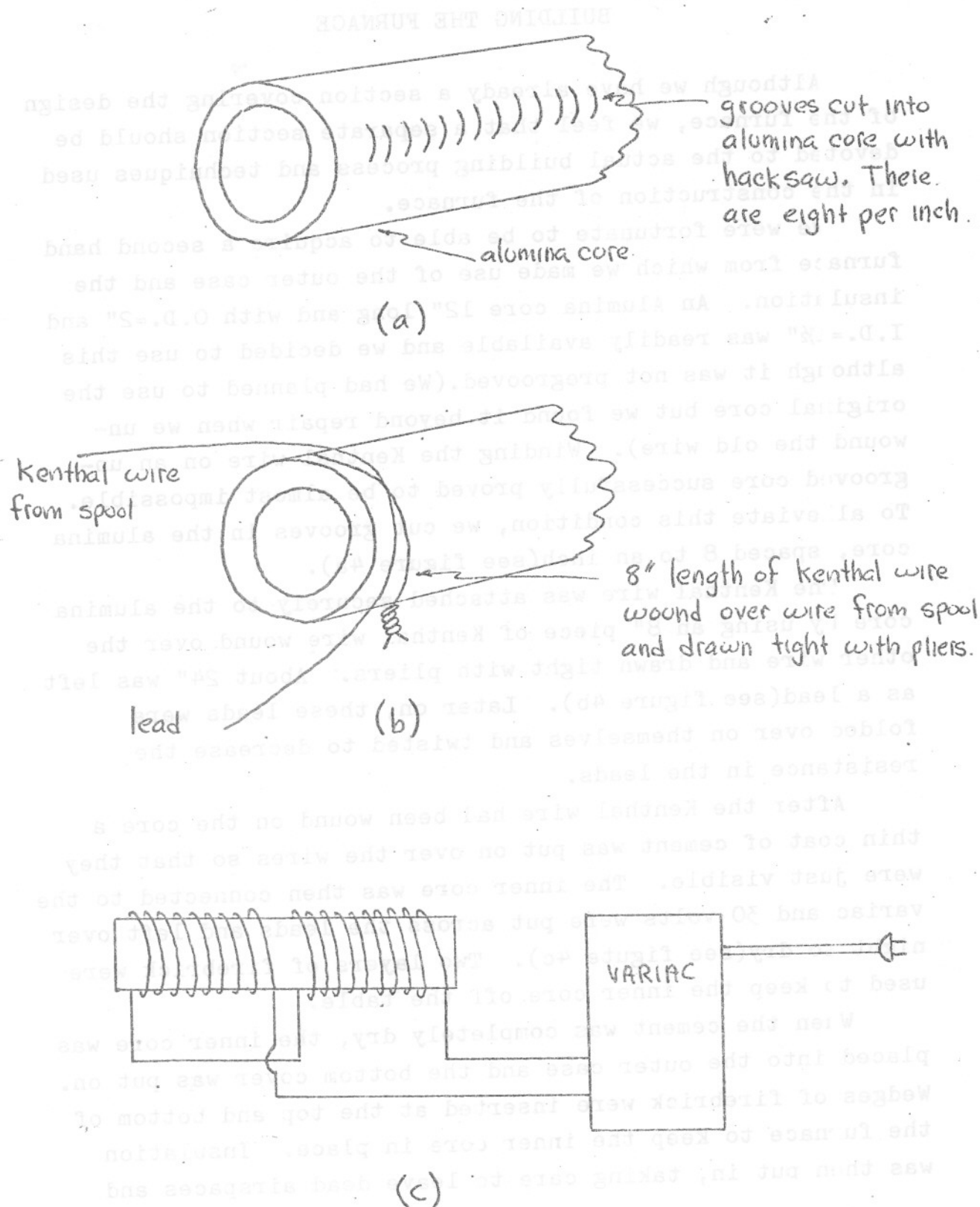


FIGURE (4)

A piece of firebrick was cut into cylindrical shape about  $1 \frac{3}{8}$ " in diameter and  $4 \frac{3}{4}$ " long. A groove was cut in its side to accommodate thermocouple #1's leads and a small hole  $\frac{1}{2}$ " in diameter and  $1/16$ " deep cut in its top into which the dilatometer fits to keep it from wobbling. See figure below:

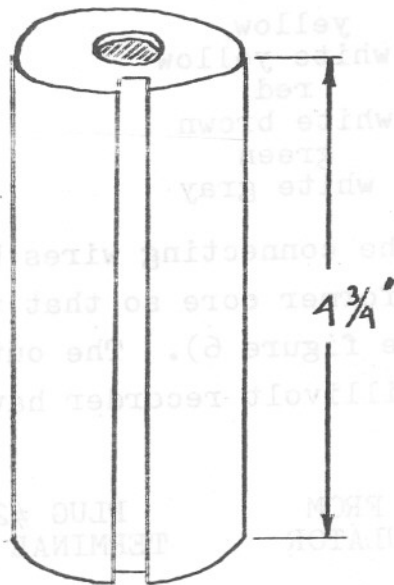


FIGURE (5)



FIGURE (6)

## LVDT CONNECTING WIRE HOOKUP

Since the leads that were connected to the transformer core were too short, additional connecting wires were soldered to them. Since the connecting wires were not all of the same color code as the wires from the transformer core, the following convention was established.

WIRES FROM LVDT TRANSFORMER CORE	CONNECTING WIRES	DEMODULATOR TERMINAL #s	PLUG#1 TERMINAL #s
yellow-black	yellow	#3	#3
yellow-red	white yellow	#4	#4
red	red	#5	#5
blue	white brown	#6	#6
green	green	#7	#7
black	white gray	#8	#8

Plug #1 was inserted in the connecting wires between the demodulator and the transformer core so that the two could be easily disconnected (see figure 6). The output wires and connecting wires to the millivolt recorder have the following convention:

DEMODULATOR TERMINAL #s	WIRES FROM DEMODULATOR	PLUG #2 TERMINAL #s	CONNECTING WIRES TO MILLIVOLT RECORDER
#9	white yellow	#1	black (common)
#10	white brown	#2	green (- unfiltered)
#11	white gray	#3	red (+ filtered)

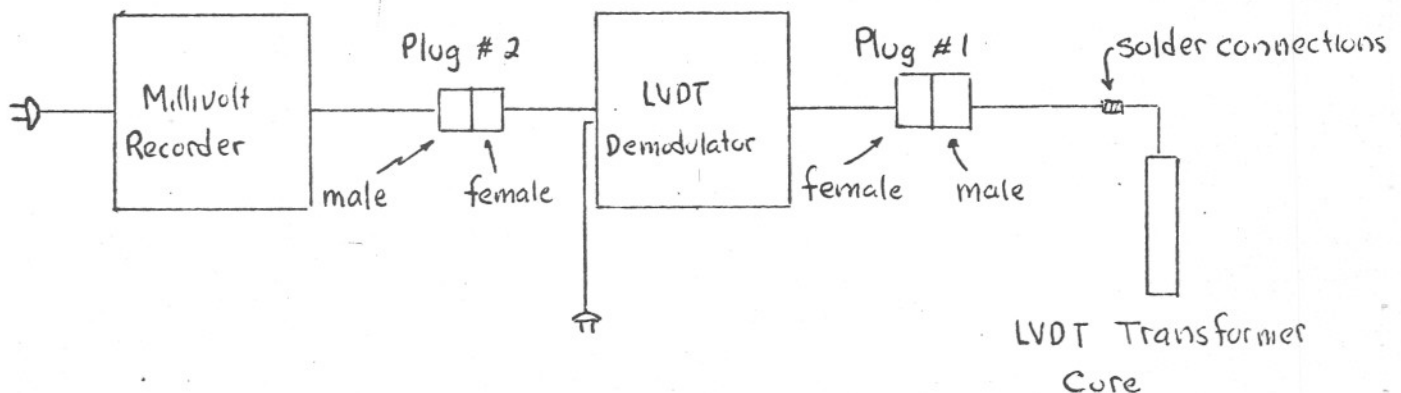


FIGURE (6)



## CALIBRATION PROCEDURE

The millivolt servo-recorder-LVDT system will be calibrated by the two methods described below.

### CALIBRATION I

A) Two samples, each 1/8" in diameter and of different lengths (approximately between 1/2" and 3/8") will be placed into the dilatometer separately after all experimental apparatus has been set-up and ready to perform.

(Note: Ends of samples must be made perfectly flat in order that experimenter may be assured that length is uniform.)

B) Position of millivolt recorder will be recorded in each case.

This procedure allows us to obtain the calibration of the system, i.e., the change in x unit length = change in y millivolts.

### CALIBRATION II

A sample of known composition is placed in the dilatometer. (1/8" diameter, about 1/2" length) An actual experimental run is performed and the data obtained is compared with that of the best known data for that particular composition. This will therefore allow us to determine the error of our apparatus.

(Note: See "Experimental Procedure" for exact details of experimental run.)

Each bundle of leads coming from the LVDT demodulator to the two female plugs is approximately 6" long. The connecting wires to the millivolt recorder is approximately 24" long. The connecting wires to the transformer core is approximately 60" long.

## CALIBRATION I

(A) Two samples, each  $1/8$ " in diameter and of different lengths (approximately between  $1/2$ " and  $3/8$ ") will be placed into the dilatometer separately after all experimental apparatus has been set-up and ready to perform. (Note: Ends of samples must be made perfectly flat in order that experimenter may be assured that length is uniform.)

(B) Position of millivolt recorder will be recorded in each case.

This procedure allows us to obtain the calibration of the system, i.e., the change in x unit length-change in y millivolts.

## CALIBRATION II

A sample of known composition is placed in the dilatometer.  $1/8$ " diameter, about  $1/2$ " length. An actual experimental run is performed and the data obtained is compared with that of the best known data for that particular composition. This will therefore allow us to determine the error of our apparatus.

(Note: See "Experimental Procedure" for exact details of experimental run.)



The copper slug is then attached to the pushrod as seen in figure 1. This assembly is inserted into the furnace and clamped into place by a rigid external clamping system. Next, the LVDT demodulator is turned on and the initial positions of the millivolt recorder and the temperature recorder are noted.

(Note: The millivolt recorder may be adjusted to zero millivolts at this point in order to have more range. This may be done by loosening the allen screw on top of the pointer mechanism and moving the pointer to zero.)

The time proportioning control is preset to a maximum temperature that the furnace is to obtain.

Simultaneously, the temperature recorder chart drive, millivolt recorder chart drive, time proportioning controller and variac are turned on.

(Note: The variac control knob is initially set at zero and is then brought up to 120 volts; this will avoid a large current impulse).

This operating condition is continued until the final temperature is obtained. At this point the experimental run will be completed.

From the data of calibration I, a known specific change in millivolts on the recorder will correspond to a specific change in length. (Refer to Calibration I). Therefore, from the recorded data we can establish a one to one correspondence between the temperature of the sample and its length at that temperature. From this information, a plot of linear thermal expansion (i.e.  $\Delta l/l$ , where  $\Delta l$  represents the change in length from the initial to the final temperature and  $l$  represents the length at the initial temperature) in percent may be made versus temperature (figure 8). It is therefore possible to make a straight line approximation to the curve for a small temperature interval and obtain the coefficient of linear expansion for that particular interval.

APPENDIX A

APPARATUS MANUFACTURER'S AND MODEL NUMBER

QUANTITY	INSTRUMENT	MODEL #	MANUFACTURER
1	Variac	W10MT3	
1	Millivoltserve Recorder	E-6701	Esterline Angus
1	Time Proportioning Controller	715	API Instruments
1	Temperature Servo Recorder	6704	Esterline Angus
1	LVDT	DMPS-3	Schaevitz Engineering Co.
2	Thermocouple	Chromel (+) Alumel (-)	-----
1	Millivolt Potentiometer	8686	Leeds and Northrup
-	Wire	18 gauge	Kenthal

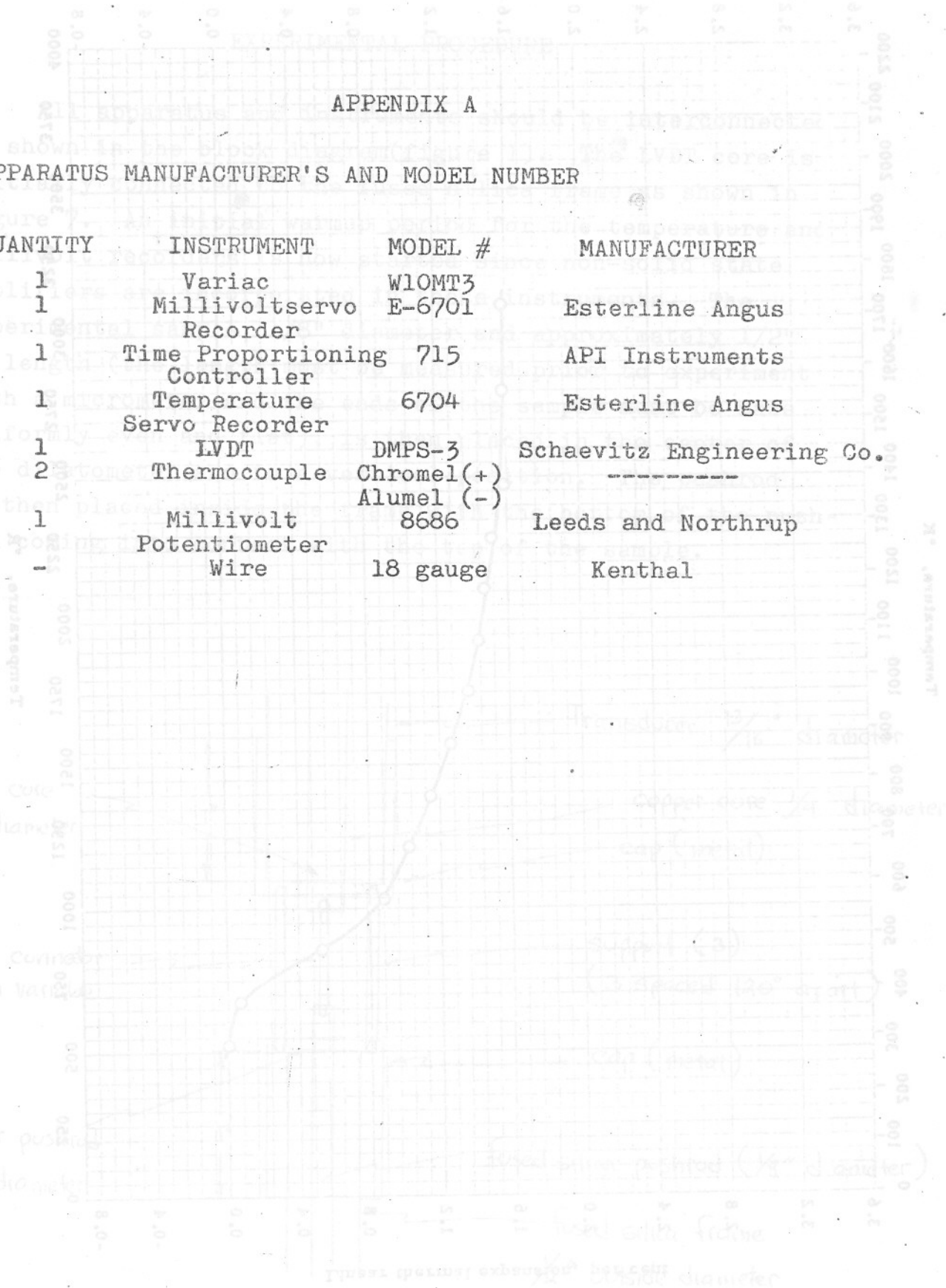


FIGURE (A)

APPENDIX B

A dilatometer is used to measure the coefficient of expansion of various materials. The instrument used in this experiment was originally designed to operate between 77°K to 1000°K, but because of problems developed in reading the sample from here, only the higher temperature regions were used (300°-1000°K). A Linear Variable Differential Transformer (LVDT) was used as an effect.

OPERATION AND CALIBRATION OF A DILATOMETER

By

Siegfried Esslinger

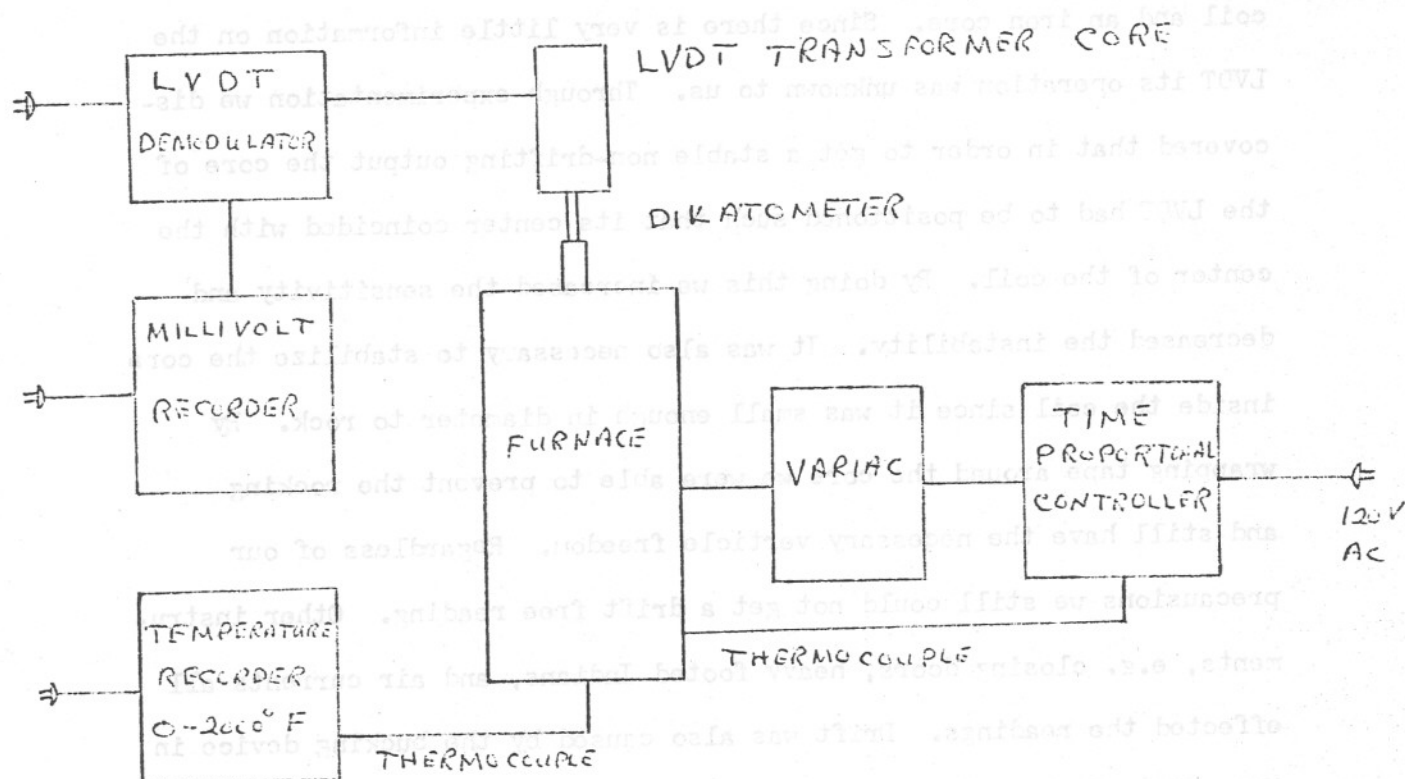
Walter Werner

### ABSTRACT

A dilatometer is used to measure the coefficient of expansion of various materials. The instrument used in this experiment was originally designed to operate between  $77^{\circ}\text{K}$  to  $1000^{\circ}\text{K}$ , but because of problems developed in sealing the sample from the atmosphere, only the higher temperature regions were used ( $300^{\circ}$ - $1000^{\circ}\text{K}$ ). A Linear Variable Differential Transformer (LVDT) was used to convert the expansion to an electrical signal which was amplified and recorded on a mv recorder. After the initial problems of the LVDT (which will be discussed later) were solved we were able to calibrate and convert the millivolt deflection to inches of expansion. We kept an accurate account of the temperature using a potentiometer which allowed us to plot expansion vs temperature.

### OPERATION OF DILATOMETER

Figure (A) shows a block diagram of the dilatometer.



The voltage supplied to the oven is controlled by a variac which allows us to slow down or speed up the heating as desired. Originally the apparatus included a time proportional control, but because of the high sensitivity of the LVDT it was of no use since it caused considerable disturbance in the millivolt reading. The furnace was allowed to heat up continuously at a given rate determined by the variac.

An Easterline Angus temperature recorder was used to monitor the heating rate, but it was not used to measure the temperature directly. We found it more convenient as well as accurate to use a Potentiometer.

The thermocouple (chromelalumel) was positioned next to the sample rather than inside the sample as is the nature of some dilatometers.

The LVDT was used to measure the expansion. It is composed of a coil and an iron core. Since there is very little information on the LVDT its operation was unknown to us. Through experimentation we discovered that in order to get a stable non-drifting output the core of the LVDT had to be positioned such that its center coincided with the center of the coil. By doing this we increased the sensitivity and decreased the instability. It was also necessary to stabilize the core inside the coil since it was small enough in diameter to rock. By wrapping tape around the core we were able to prevent the rocking and still have the necessary verticle freedom. Regardless of our precautions we still could not get a drift free reading. Other instruments, e.g. closing doors, heavy footed Indians, and air currents all effected the readings. Drift was also caused by the bucking device in the millivolt recorder which had to be adjusted to give the deflection before each run.

By keeping things the same as possible for each run we were able to get relatively reproducible runs. The different runs have been plotted on the graphs at the end.



### CALIBRATIONS

Once the LVDT was stabilized to a 10% drift over a one half hour period, we took a sample of aluminum (0.483 inches long) and placed it in the dilatometer. We thus used aluminum as our standard. The expansion of aluminum recorded by the deflection of the mv recorder could then be related to the calculated expansion.

$$\Delta L = \alpha L \Delta T$$

$\Delta L$  = Change in length due to expansion.

L = Length of sample.

$\Delta T$  = Change in temperature.

$\alpha$  = Coefficient of linear expansion.

For aluminum:

Temp. °C	$\alpha$
20 - 100	$23.26 \times 10^{-6}$
20 - 200	$24.58 \times 10^{-6}$
20 - 300	$25.45 \times 10^{-6}$
20 - 400	$26.49 \times 10^{-6}$
20 - 500	$27.43 \times 10^{-6}$

We took the maximum deflection and divided it into the maximum expansion which gave us the inch equivalent of the millivolt change. Provided we kept everything the same all drift and glass expansion were accounted for by the calibration.

We performed two different heating rate experiments because at low temperature the sample does not have time to acclimate to the surrounding temperature. The results for the slow run prove to be more accurate than the fast run results, but the rate was limited by the drifting effect which became too appreciable at slow rates.

The results were:

A. <u>Fast runs at 120 volts</u>		
	<u>Inch/Div</u>	<u>Error</u>
7	.5362x 10 <sup>-5</sup>	.0092
8	.5454x 10 <sup>-5</sup>	.0001
9	.6026x 10 <sup>-5</sup>	.0576
10	.4981x 10 <sup>-5</sup>	.0573
<u>Average value:</u>	54.55 x 10 <sup>-7</sup> ± .0472 x 10 <sup>-5</sup>	inches/unit deflection *
B. <u>Slow runs at 90 volts</u>		
	<u>Inch/Div</u>	<u>Error</u>
11	.6296x 10 <sup>-5</sup>	.0465
12	.6877x 10 <sup>-5</sup>	.0116
13	.7109x 10 <sup>-5</sup>	.0348
<u>Average value</u>	67.6 x 10 <sup>-7</sup> ± 4.39 x 10 <sup>-7</sup>	inches/unit deflection

From these values we were able to plot the expansion of steel (fast) and ferrite (slow) and from the slope of the  $\Delta L/L$  vs T graphs we can find the coefficients of thermal expansion:

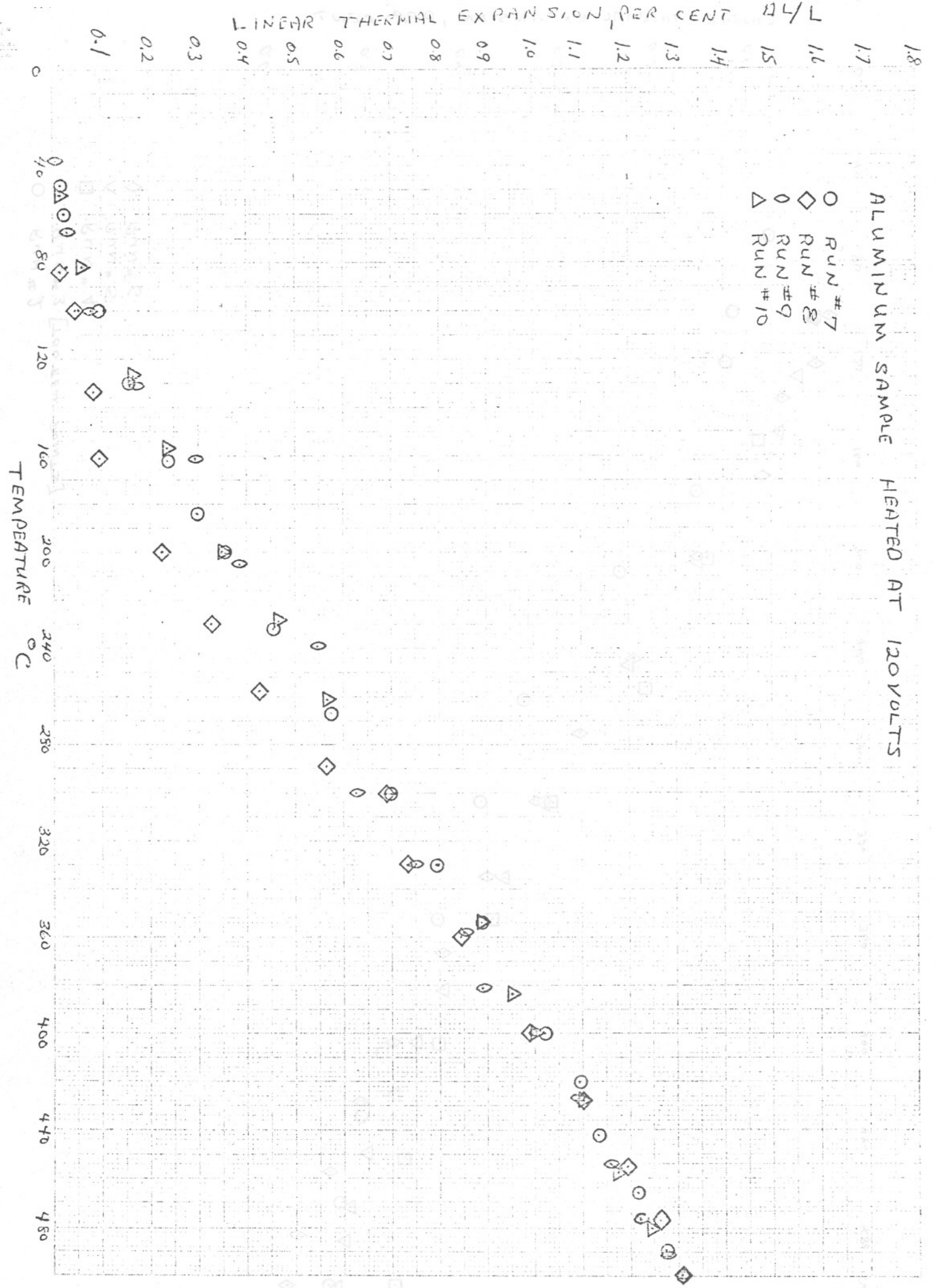
For steel:  $\alpha = \frac{5.5 \times 10^{-3}}{473} = 10.6 \times 10^{-6} \pm .46 \times 10^{-6}$

For ferrite:  $\alpha = \frac{.92 \times 10^{-3}}{723} = 13.08 \times 10^{-6} \pm .65 \times 10^{-6}$

\*Each division in our calibration was equal to .06 inches, which is also a unit deflection.

ALUMINUM SAMPLE HEATED AT 120 VOLTS

- RUN #7
- ◇ RUN #8
- ◊ RUN #9
- △ RUN #10



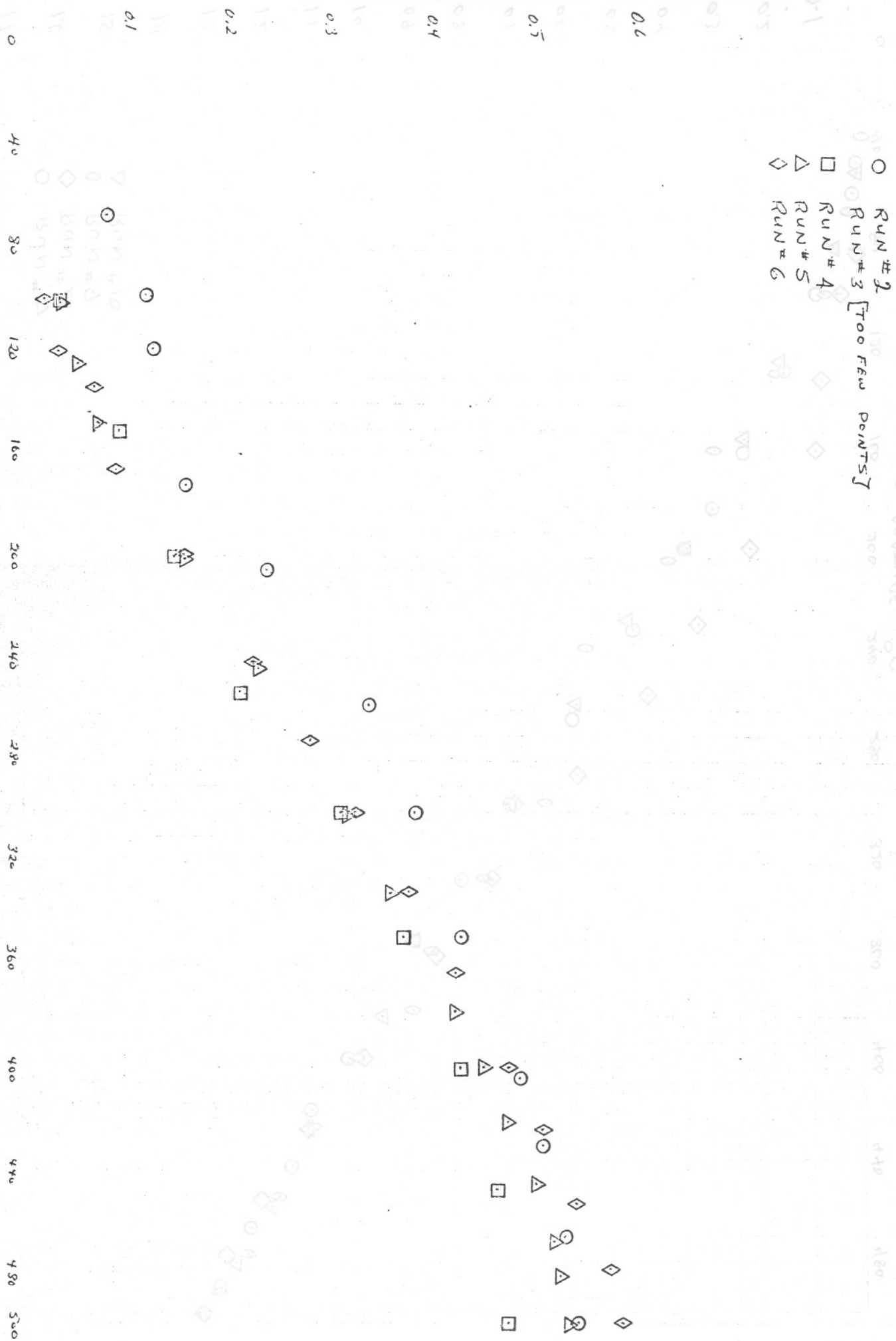
CORDED STEEL HEATED AT 150 VOLTS

ROLLED STEEL HEATED AT 120V OLTS

LEVERAGE

- RUN # 2
- RUN # 3 [Too few points]
- △ RUN # 4
- ◇ RUN # 6

LINEAR THERMAL EXPANSION, PER CENT

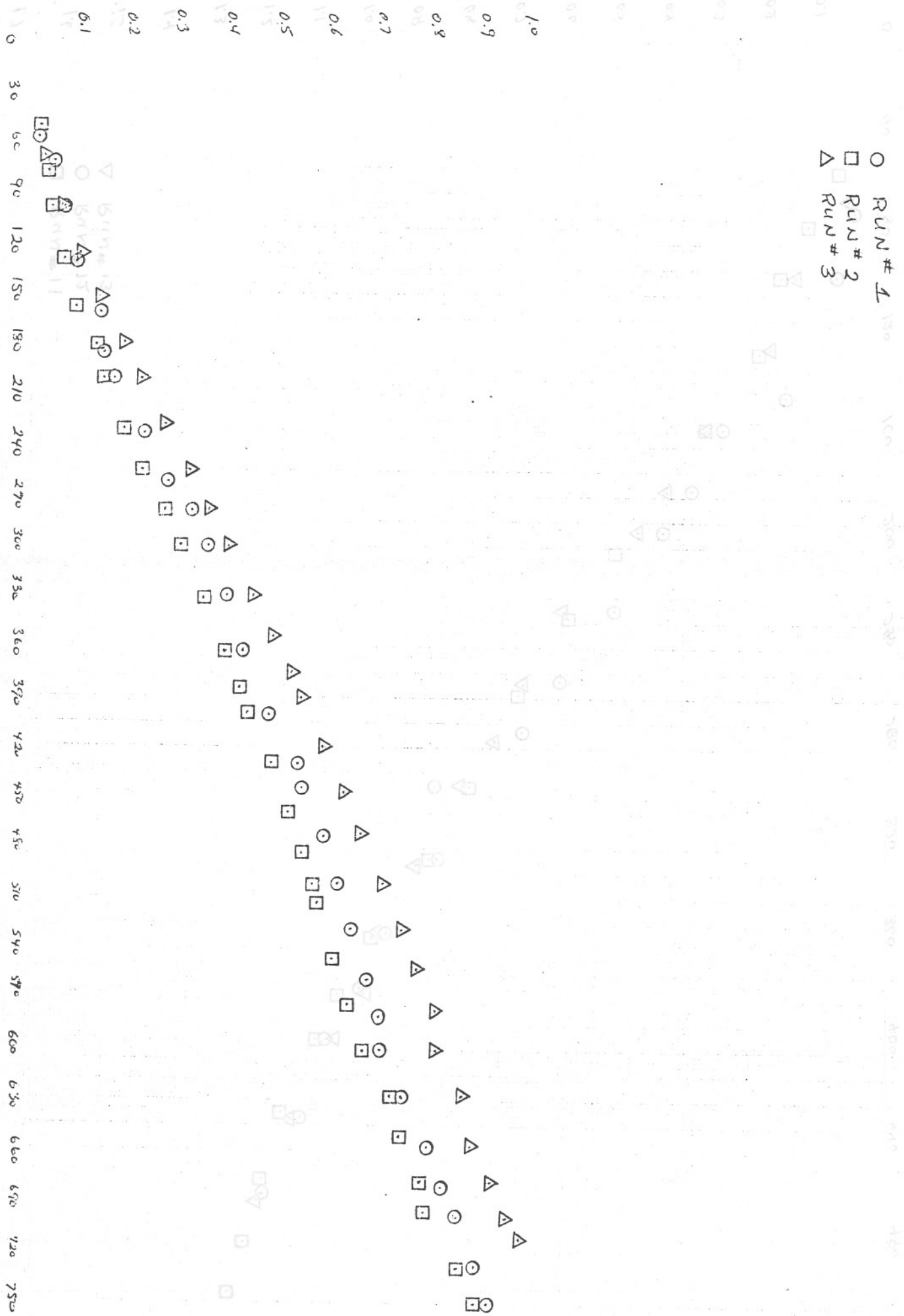


FERRITE SAMPLE HEATED AT V=90 VOLTS

LEWISVILLE, OH

- RUN # 1
- RUN # 2
- △ RUN # 3

LINEAR THERMAL EXPANSION, PER CENT



LEWISVILLE, OH

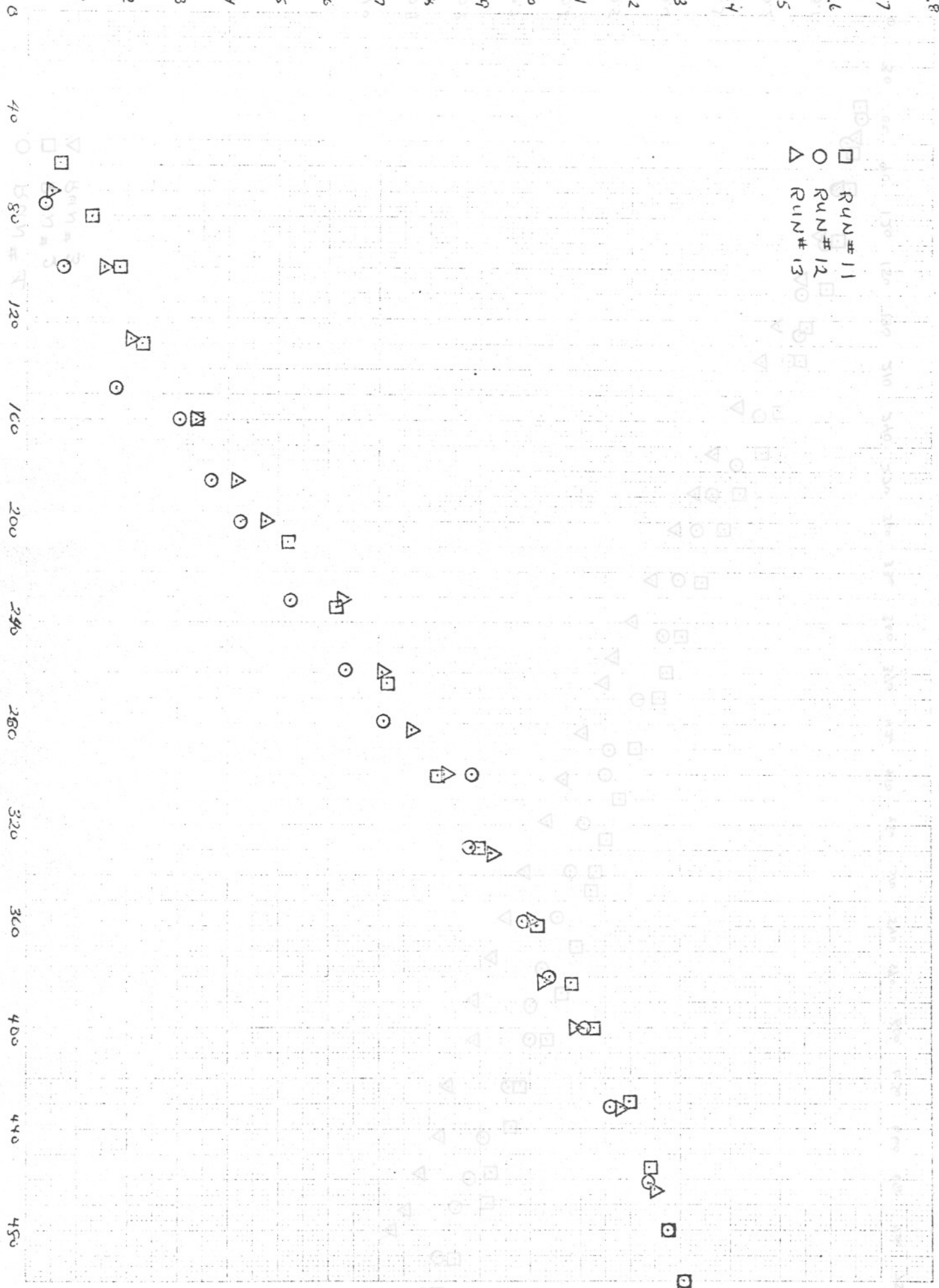
ALUMINUM SAMPLE HEATED AT 1-KV VOLTS

LINEAR THERMAL EXPANSION, PER CENT

1.8  
1.7  
1.6  
1.5  
1.4  
1.3  
1.2  
1.1  
1.0  
0.9  
0.8  
0.7  
0.6  
0.5  
0.4  
0.3  
0.2  
0.1

□ RUN # 11  
○ RUN # 12  
△ RUN # 13

TEMPERATURE °C



FERRITE 20 WOL% HEATED AT 1-KV VOLTS



APPENDIX C

Abstracts of Presented Talks

Time on Program	Title	Author
1:00-2:15 P.M.	Elastic Moduli of Binary Composites	L. M. Barker, Dept. of Materials Science, State University of New York at Stony Brook, Stony Brook, New York 11790
	<p>A theory is presented here to relate the elastic moduli of the two phase composite to the elastic properties of its constituents. The theory is based on the variational approach advanced by Hashin and Shtrikman. Types of dislocations and particle shape of the dispersed are treated in a statistical manner. The agreement between the theory and the experimental results such as the work in Al<sub>2</sub>O<sub>3</sub> in 1960, in Y<sub>2</sub>O<sub>3</sub> in glass, and other binary systems are found to be good.</p> <p>(This work is partially supported by the National Aeronautics and Space Administration, Electronic Research Center, Cambridge, Mass. Grant No. 33-615-082)</p>	

Time on Program: 2:00-2:15 P.M.

Title: Elastic Moduli of Binary Composites

Author: Franklin F.Y. Wang Dept. of Materials Science

State University of New York at Stony Brook, Stony  
Brook, New York 11790

Abstract:

A theory is presented here to relate the elastic modulus of the two phase composite to the elastic properties of its constituents. The theory is based on the variational approach advanced by Hashin and Shtrikman. Types of dispersions and particle shape of the dispersant are treated in a statistical manner. The agreement between the theory and the experimental results such as the pores in  $Al_2O_3$ , in  $MgO$ , in  $Y_2O_3$ , in glass, and other binary systems are found to be good.

(This work is partially supported by the National Aeronautics and Space Administration, Electronic Research Center, Cambridge, Mass. Grant No. 33-015-085).

Abstract Submitted  
for the March Meeting of the  
American Physical Society

January 2, 1969

Physical Review  
Analytic Subject Index  
Number 49.8

Bulletin Subject Heading  
in which Paper should be placed  
Ferroelectrics

Empirical Factors for Calculation of the Ferroelectric  
Transition Temperatures of Tungsten Bronze Type Niobates.\*

F. F. WANG, Department of Materials Science, State University  
of New York, Stony Brook, New York. Recently, it was found  
that the ferroelectric transition temperatures (Curie temp-  
eratures) can be correlated with the atomic displacements <sup>1</sup>  
in displacive ferroelectrics, and the axial ratios <sup>2</sup> in the  
niobates with a tungsten bronze structure. This paper re-  
ports on an approach, based on the lattice dynamical theory  
of ferroelectricity, to obtain empirical factors for cal-  
culation of Curie temperatures in tungsten bronze type  
niobates. These factors are obtained for cations such as  
alkalis, alkaline earths, lead and lanthanum. The agree-  
ments between calculations and experimental data are good.

\*Supported in part by the National Aeronautics and Space  
Administration, Electronic Research Center, Cambridge,  
Mass. (Grant No. 32-015-085).

1. S.C. Abrahams, S.K. Kurtz, and P.B. Jamieson, Phys.  
Rev. 172, 551 (1968).
2. E.A. Giess, B.A. Scott, G. Burns, D.F. O'Kane, and  
A. Segmüller, J. Am. Ceram. Soc. 1969 (to be published).

APPENDIX D

Empirical Factors for Calculation of  
the Ferroelectric Transition Temperatures of  
Tungsten Bronze Type Niobates\*

January 2, 1969

Franklin F. Y. Wang

Department of Materials Science  
State University of New York  
Stony Brook, New York

Physical Review  
Analytic Subject Index  
Number 1.8

Bulletin Subject Heading  
in which Paper should be placed  
Ferroelectrics

Empirical Factors for Calculation of the Ferroelectric  
Transition Temperatures of Tungsten Bronze Type Niobates.  
F. F. WANG, Department of Materials Science, State University  
of New York, Stony Brook, New York

Abstract

This present work correlates  $T_c$  directly to the chemical compositions of the tungsten bronze type niobates and it was found that the compositional effect can be additively considered.

\*Supported in part by the National Aeronautics and Space Administration, Electronic Research Center, Cambridge, Mass. (Grant No. NS-412-082).

J. S. C. Abraham, S. K. Kurta, and P. B. Jamieson, Phys. Rev. 175, 751 (1968).

S. E. A. Glass, B. A. Scott, G. Burns, D. V. O'Kane, and A. Szafraniec, J. Am. Ceram. Soc. 1969 (to be published).

Recently, Abrahams et al (1968) found a quadratic relationship between  $T_c$ , ferroelectric transition temperature, and  $\Delta z$ , the atomic displacement by the homopolar metal atom along the polar axis at  $T \ll T_c$ , in many displacive ferroelectrics. Giess et al (1969) found that for the niobates of the tungsten bronze type, linear relationships exist between  $T_c$  and  $c/a$ , the lattice parameter axial ratios of the compounds. This present work correlates  $T_c$  directly to the chemical compositions of the tungsten bronze type niobates and it was found that the compositional effect can be additively considered.

The approach is based on the lattice dynamical theory of ferroelectricity. We adopt a one dimensional lattice of the polyatomic molecule, following Brillouin (1953). Within each cell of this linear molecule,  $NbO_3$  is treated as a single entity as are the other cations. This is appropriate because  $NbO_6$  octahedra in niobates are linked through corners and each oxygen is shared between two octahedra. A wave solution of the atomic displacement is assumed. The square of the frequency  $\omega^2$  is a linear function of  $T - T_c$ , as shown by Silverman (1964), i.e.,  $(1/A)\omega^2 = (T - T_c)$  where  $A$  is a function of  $M_r$ , the mass of the  $r$ -th atom within each cell. The function  $D_{r,s}(k)$  is defined as:

$$D_{r,s}(k) = \sum_p C_{prs} e^{-ikp} \text{ for } r \neq s; \text{ and}$$

$$D_{r,r}(k) = - \sum_{ps} C_{prs} + \sum_p C_{pr} e^{-ikp}. \quad C_{prs} \text{ is the interaction}$$

constant on atom  $r$  in cell  $n$  due to atom  $s$  in cell  $n+p$ . Each compound has different  $A$  and  $T_c$  values. By assuming that  $\omega$  is nearly the same for isostructural compounds, the compositional correlation should, therefore, exist between  $1/A$  and  $T_c$ .

For the first approximation, we replace  $1/A$  by  $1/(\sum_r X_r D_{rr}/M_r)$  where  $X_r$  is the mole fraction of the cation in the compound. We assume a linear relationship between it and  $T_c$ , such as

$$1/(\sum_r X_r D_{rr}/M_r) = C T_c + D \quad (1)$$

From the known  $T_c$  values (Giess et al, 1969; O'Kane et al 1968; VanUitert et al 1968) of tungsten bronze type niobates, the general constant  $C$  and  $D$  and the empirical factors  $D_{rr}$  for various cations can be obtained through a series of successive numerical iterations. In some cases, convergence was not obtained. Arbitrary truncation was introduced to reduce the  $\Delta T_c$  between experiment and calculation and to maximize the number of niobates with small  $\Delta T_c$  values. The constants  $C$  and  $D$  were found to be 1.169 and -4.09, respectively. The determined empirical factors  $D_{rr}$  for various cations are listed in Table 1. The larger  $D_{rr}/M_r$  value has the effect of lowering the Curie point.

Using these factors, the  $\Delta T_c$  values between experiment and calculation for some niobates are listed in Table 2. A  $\Delta T_c$  of  $\pm 15^\circ$  is considered to be in good agreement. It is clear, from Table 2(a), that the same set of empirical factors will produce good agreement in some compounds and poor agreement in others. As shown in Table 2(b), the factors for



K, Ba, Sr, and La produced fair agreement. However, the factor for Pb was poor, and the combination of Pb and La produced the worst  $\Delta T_c$  values. In such cases, it is probably due to significant local structural distortions from the cation substitutions.

As shown by Jamieson et al (1968) there are ten  $NbO_6$  octahedra in a unit cell of the tungsten bronze structure. Among the octahedra, they can contain up to ten cations sites. Two A1 (or  $\alpha$ ) sites are 12-coordinated cubo-octahedral; four A2 (or  $\beta$ ) sites are 9-coordinated tricapped trigonal prismatic; and four C (or  $\gamma$ ) sites are 3-coordinated planar trigonal. Most of the niobates have their A1 and A2 sites filled by cations. For example, in  $Ba_2Na(NbO_3)_5$ , Na atoms fill the A1 sites, and Ba atoms fill the A2 sites. In some of the Li-containing niobates, such as  $K_3Li_2(NbO_3)_5$ , K atoms fill the A1 and A2 sites, and Li fills the C sites. As shown in Table 2(c), this C-sites occupancy of Li produced poor agreement in  $T_c$  values. When the C-site occupancy of Li is smaller in proportion, as in the case of  $xNaBa_2(NbO_3)_5 \cdot (1-x)Na_3Li_2(NbO_3)_5$  with  $x=0.8$ , the agreement becomes good. This illustrates the sensitivity of the empirical factors to the type of site occupancy. When the factors are applied to niobates of perovskite structure as in Table 2(d), the agreement is very poor.

We have applied the factors to 34 niobates of tungsten bronze type. We found that 32.4% of the niobates have

$|\Delta T_c|$  of  $\leq 10$ ; 44.1%tile for  $\leq 15$ ; 76.5%tile for  $\leq 50$ ; and 85.3%tile for  $\leq 90$ . It is therefore concluded that these factors can be considered as operational. They can predict the Curie point within reasonable range, and they are sensitive to structural differences. Moreover, they can be useful in providing, on an arbitrary scale, the interaction constants between atoms in these niobates.

Bibliography

Acknowledgment

\* Supported in part by The National Aeronautics and Space Administration, High Altitude Research Center, Cambridge, Massachusetts (Grant No. 33-012-082)

The author wishes to thank Drs. Giess and Abrahams for communicating their results prior to publication.

Abrahams, S. G., Kopp, E. K., and Jamieson, H. F. (1968) *Phys. Rev.*

Giess, S. A., Scott, R. A., Burns, D. P., O'Kane, D. P., and Sengulifer, A. (1969) *J. Nucl. Energy, Sec. C*

Jamieson, H. F., Abrahams, S. G., and Bernstone, J. D. (1968) *J. Chem. Phys.*

O'Kane, D. P., Burns, D. P., Scott, R. A., and Giess, S. A. (1968) *J. Electrochem. Soc.*

Silverman, R. E. (1964) *Phys. Rev.*

Yasufert, I. G., Levinstein, H. J., Rubin, J. M., Caplan, C. D., Dearborn, E. P., and Connor, V. A. (1968) *Mar. Res. Bull.*

## Bibliography

\* Supported in part by The National Aeronautics and Space Administration, Electronic Research Center, Cambridge, Massachusetts (Grant No. 33-015-085)

Abrahams, S.C., Kurtz, S.K., and Jamieson, P.B. (1968).  
Phys. Rev. 172, 551.

Brillouin, L. (1953). Wave Propagation in Periodic Structures,  
p. 65, New York, Dover.

Giess, E.A., Scott, B.A., Burns, G., O'Kane, D.F. and  
Segmüller, A. (1969). J. Am. Ceram. Soc.

Jamieson, P.B., Abrahams, S.C., and Bernstein, J.L. (1968).  
J. Chem. Phys. 48, 5048.

O'Kane, D.F., Burns, G., Scott, B.A., and Giess, E.A. (1968).  
J. Electrochem. Soc. 115, 1081.

Silverman, B.D. (1964). Phys. Rev. 135, A1596.

VanUitert, L.G., Levinstein, H.J., Rubin, J.J., Capio,  
C.D., Dearborn, E.F., and Bonnor, W.A. (1968). Mat.  
Res. Bull. 3, 47.

Table 1

Empirical Factors and Constants

Constants:

$C = 1.169$

$D = -4.09$

Empirical Factors:

	$D_{rr}$	$D_{rr}/M_r$
Li <sup>†</sup>	0.058	0.0031
Na <sup>†</sup>	0.042	0.0018
K <sup>†</sup>	0.155	0.0010
Rb <sup>†</sup>	0.424	0.0050
Ba <sup>††</sup>	0.165	0.0012
Sr <sup>††</sup>	0.361	0.0041
Pb <sup>††</sup>	0.374	0.0018
La <sup>†††</sup>	9.461	0.0068
(NbO <sub>3</sub> ) <sup>-3</sup>	0.106	0.00075



Distribution List

Copies

- |  |  |
|--|--|
| <p>1. Graduate School<br/>State University of New York at Stony Brook<br/>Stony Brook, New York 11790</p> <p>2. Office of Grants and Resources<br/>National Aeronautics and Space Administration<br/>Washington, D. C. 20546</p> <p>3. Electronics Research Center<br/>National Aeronautics and Space Administration<br/>Cambridge, Massachusetts 02139<br/>Attention: Dr. James Childress<br/>              Dr. Philip H. Kelin<br/>              Dr. Howard Lesoff<br/>              Dr. D.M. Warschauer</p> | <p>25</p> <p>25</p> <p>1<br/>1<br/>1<br/>1</p> |
|--|--|

(C)

(D)